Available online at www.sciencedirect.com
SCIENCE DIRECT®
Tectonophysics 377 (2003) 55–82
TECTONOPHYSICS
www.elsevier.com/locate/tecto

New paleomagnetic paleolatitudes for the Omulevka terrane of northeast Russia: a comparison with the Omolon terrane and the eastern Siberian platform

D.B. Stone[a,*], P. Minyuk[b,1], E. Kolosev[b,1]

[a] Geophysical Institute, University of Alaska, Fairbanks, AK 99775, USA
[b] Northeast Interdisciplinary Scientific Research Institute, 16 Portovaya St., Magadan, Russia

Received 17 November 2002; received in revised form 25 July 2003; accepted 25 August 2003

Abstract

Paleomagnetic measurements were made on samples from Silurian, Devonian, Carboniferous and Permian aged rocks from the Omulevka terrane, northeast Russia. The Omulevka terrane is a fragment of continental margin that forms a major component of the Kolyma–Omolon superterrane, a superterrane that constitutes the core of northeast Russia. All samples were collected from sites along the Taskan river, and all showed a very strong secondary overprint and in some cases more than one. With detailed thermal demagnetization, a component of magnetization that decayed towards the origin when viewed as an orthogonal plot was commonly present and showed better clustering of magnetization directions in stratigraphic coordinates. All of the sites sampled were tilted, but none had enough variation in bedding attitude to perform fold tests. Comparing data between localities was used as a pseudo fold test and indicates that in all but one case the characteristic remanent magnetization found represents a magnetization acquired very early in the history of the rock. Interpretation of these data in terms of both virtual pole positions and paleolatitude changes with time shows that the Omulevka terrane and the adjacent Omolon terrane were together at low latitudes in Silurian and Devonian time and until late Devonian their latitude was consistent with them being closely related to the Siberian Craton. Between Devonian and Permian times, the paleolatitudes of the terranes decreased and, when compared with equivalent reference paleolatitudes for the nearby Siberian platform, show a clear latitudinal separation. From Permian to Jurassic time, the Omulevka and Omolon terranes move steadily northwards, reducing the relative latitudinal separation from Siberia. By late Jurassic to early Cretaceous time, the observed and equivalent Siberian paleolatitudes are identical, indicating the accretion of the Kolyma–Omolon superterrane to the eastern Siberian continent.

Keywords: Paleomagnetism; Paleogeography; Northeast Russia; Omulevka; Omolon

1. Introduction

Northeast Russia east of the Siberian platform is made up of a collage of accreted terranes (Fig. 1). These show a marked similarity to the accreted terranes of Alaska that lie west of the North American platform (Nokleberg et al., 2001). In both cases, the northern-

* Corresponding author. Tel.: +1-907-474-7622; fax: +1-907-474-5163.
E-mail addresses: dstone@gi.alaska.edu (D.B. Stone), paleomag@neisri.magadan.ru (P. Minyuk), paleomag@neisri.magadan.ru (E. Kolosev).
[1] Tel.: +7-413-22-30681.

0040-1951/$ - see front matter © 2003 Elsevier B.V. All rights reserved.
doi:10.1016/j.tecto.2003.08.025

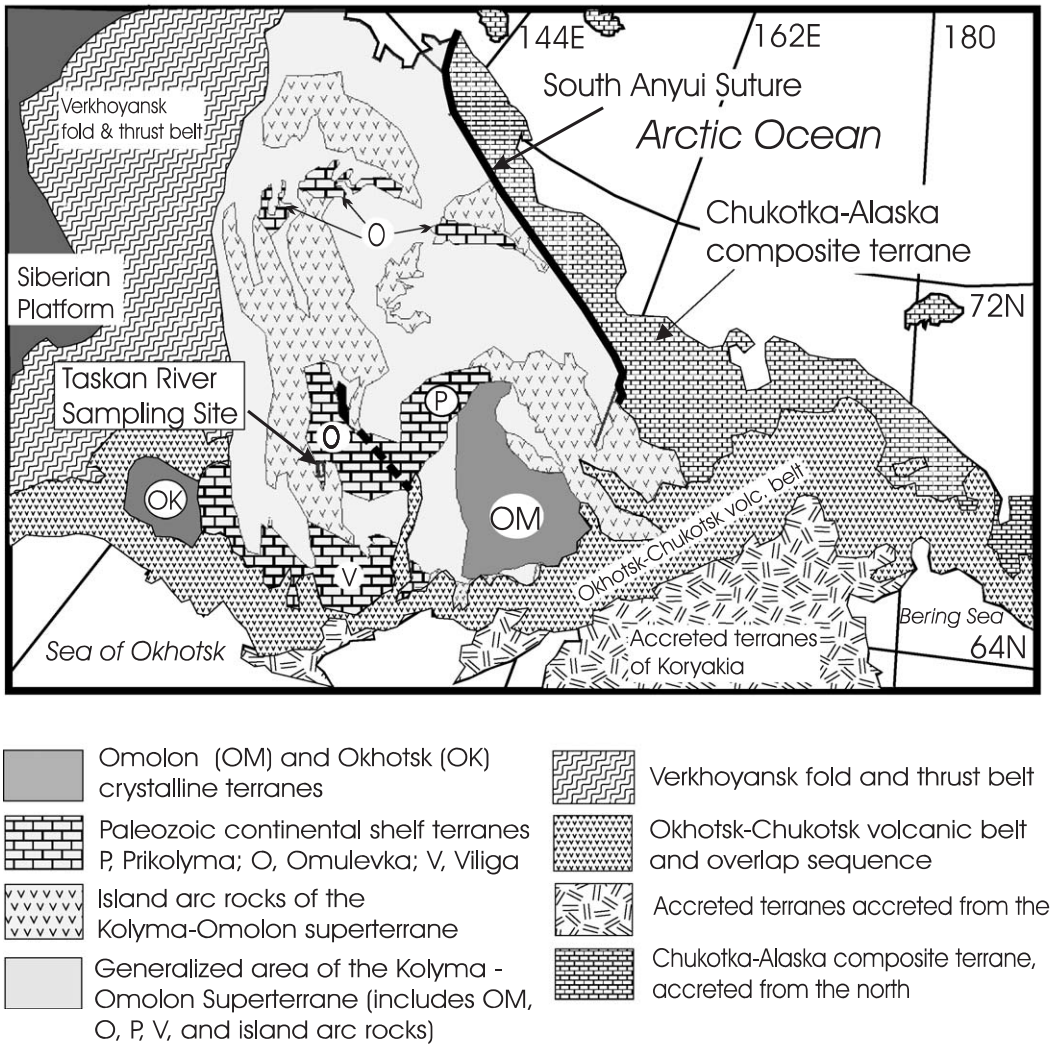

Fig. 1. A regional reference map of the tectonic components of northeast Russia. The general location of the sites sampled is shown in the Omulevka continental shelf terrane.

most terranes came from the north as the Chukotka–Alaska composite terrane rotated away from the Canadian arctic island margin (see, for instance, Lawver et al., 2002). In northeast Russia, the southern boundary of this composite terrane is marked by the South Anyui suture zone. The southeastern part of northeast Russia, including Kamchatka, was formed in late Cretaceous and later time by the accretion of terranes rafted in on the plates of the Pacific. The boundary between these latter accreted allochthonous terranes and the more inboard parts of northeast Russia is largely covered by the Okhotsk–Chukotka volcanic belt of late Cretaceous age. The western boundary of the accreted terranes of northeast Russia is the Verkhoyansk fold and thrust belt, thought to have formed in response to the collisions of the accreting terranes. The area enclosed by the Verkhoyansk fold and thrust belt, the South Anyui suture zone and the Okhotsk–Chukotka volcanic belt is known as the Kolyma–Omolon superterrane. The core of this superterrane is the Omolon massif, a terrane composed of a Proterozoic crystalline basement overlain by both Paleozoic

and Mesozoic shallow marine deposits (Nokleberg et al., 1998). Adjacent to the Omolon massif are two large fragments of Paleozoic continental margins, the Omulevka and Prikolyma terranes. Much of the rest of the Kolyma–Omolon superterrane is made up of dissected island arcs, fragments of oceanic crust, collapsed ocean basin deposits and multiple intrusive complexes.

There are many models for the tectonic history and paleogeography of the Kolyma–Omolon superterrane ranging from a paleogeography that keeps all of its component parts close to the Siberian platform at all times (Chekhov, 1990; Merzlyakov et al., 1982; Shapiro and Ganelin, 1988; Sharkovsky, 1975; Til'man, 1973) to models where the various terranes originate elsewhere and amalgamate and accrete to the platform in late Jurassic, early Cretaceous time (Nokleberg et al., 2001; Parfenov et al., 1991). The similarity of the microfossils representing Devonian and older ages on the Siberian Platform with those in the Omulevka and Prikolyma terranes led to a model requiring the terranes to remain in proximity to the platform at least for early Paleozoic time. Paleomagnetic data (Minyuk et al., 2001; Kolesov and Stone, 2002; Burke, 1984; Karasik et al., 1984; Khramov et al., 1985; Khramov and Ustrtitsky, 1990; Nokleberg et al., 1998; Parfenov, 1984, 1991; Talent, 1990; Ustritsky and Khramov, 1987; Zonenshain, 1984; Zonenshain et al., 1990a,b) suggest a compromise model involving the development of the continental margin terranes as part of the Siberian platform, after which parts of the continental margin were rifted away, and drifted several tens of degrees with respect to the parent continent. By

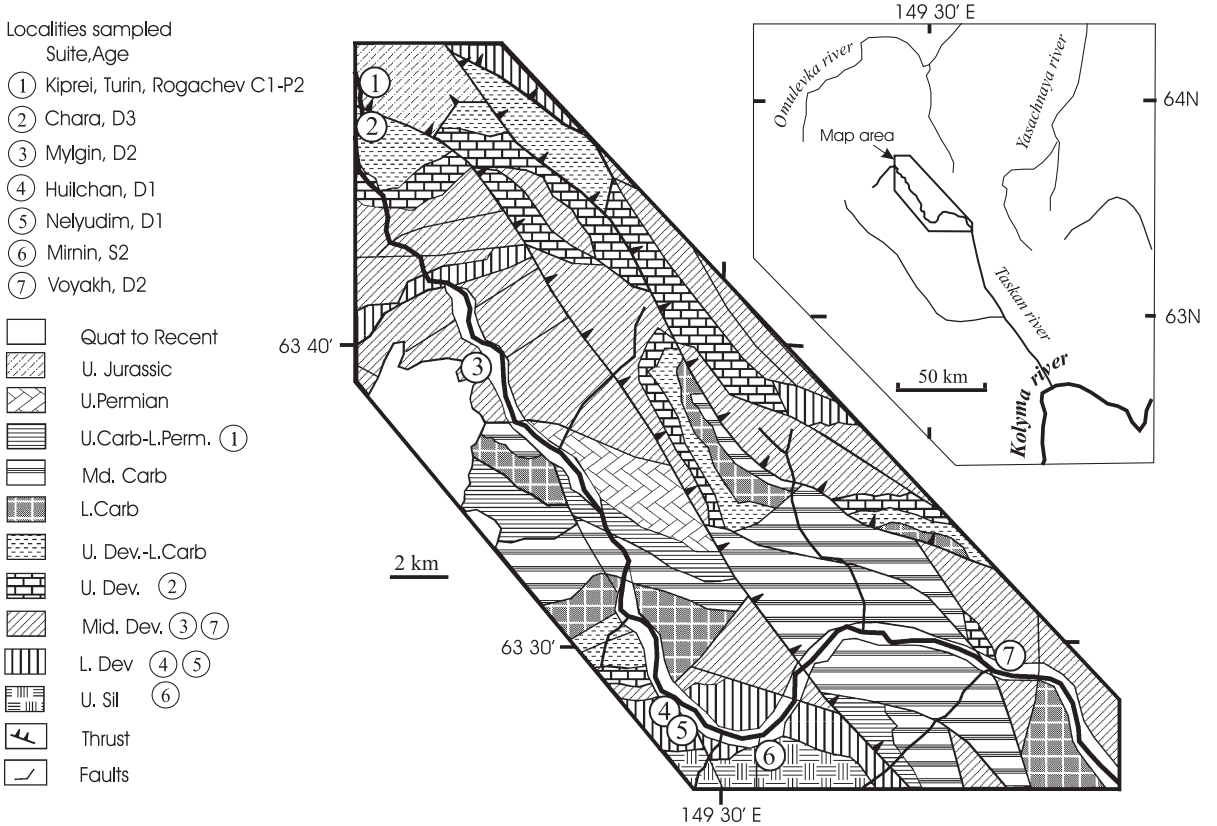

Fig. 2. Geological sketch map modified from Nikolaev (1976) showing site locations. The inset shows the location of the Taskan river with respect to the Kolyma and Omulevka rivers. All the sites sampled are on or close to the Taskan river and are shown as numbered circles. The area is complexly deformed and only representative faults are shown.

Jurassic time, they were again close to the Siberian platform and, eventually, accreted to it in late Jurassic–early Cretaceous time. This paper presents new paleomagnetic data from the Omulevka terrane that support this latter model.

2. Sampling locations

The new paleomagnetic data reported here are all from samples collected in the Omulevka terrane, which is also known as the Omulevka uplift. The Omulevka uplift is a large horst-like tectonic block confined on all sides by faults. It is a composite part of the Kolyma–Omolon superterrane (Nokleberg et al., 1998; Grinberg et al., 1981; Merzlyakov, 1966, 1986). The In'yali–Debin synclinorium lies to the south and southwest of the Omulevka uplift, and overlaps deposits associated with the Moma–Zyryan trough cover the northwestern margin. On the eastern side, it borders on the Prikolyma uplift (Gagiev, 1995). There are few paleomagnetic data from the Omulevka uplift. In the northern parts, Paleozoic rocks from the Bulkut

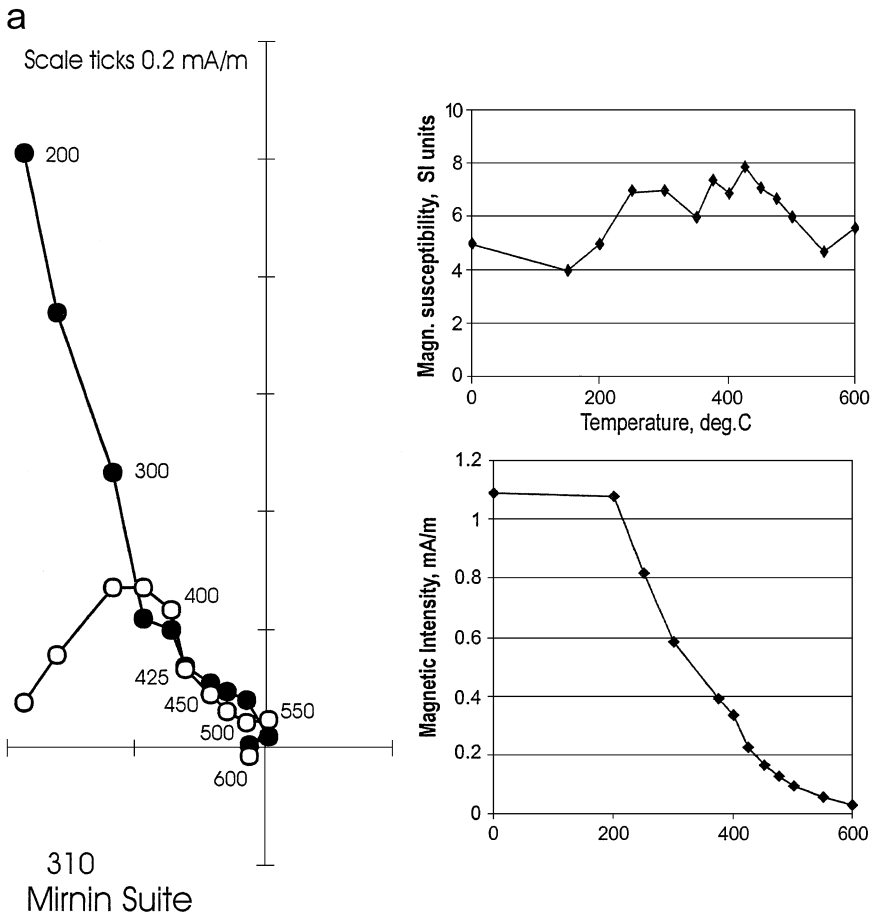

Fig. 3. Demagnetization plots for samples from the Mirnin suite of upper Silurian age. For the orthogonal vector (Zijderveldt) plots, the solid symbols represent projections onto the horizontal plane and open symbols onto the vertical plane. All diagrams are in stratigraphic (tilt corrected) coordinates unless labeled as being in Geographic coordinates (not tilt corrected). The top of the vertical axis represents North and Up, and the horizontal axis represents E–W. For thermal demagnetizations, the variations in the magnetic susceptibility and the intensity are also shown. All temperatures are in °C. Sample numbers are shown in the bottom left corner of the vector plot. (a) Sample 307, (b) sample 310.

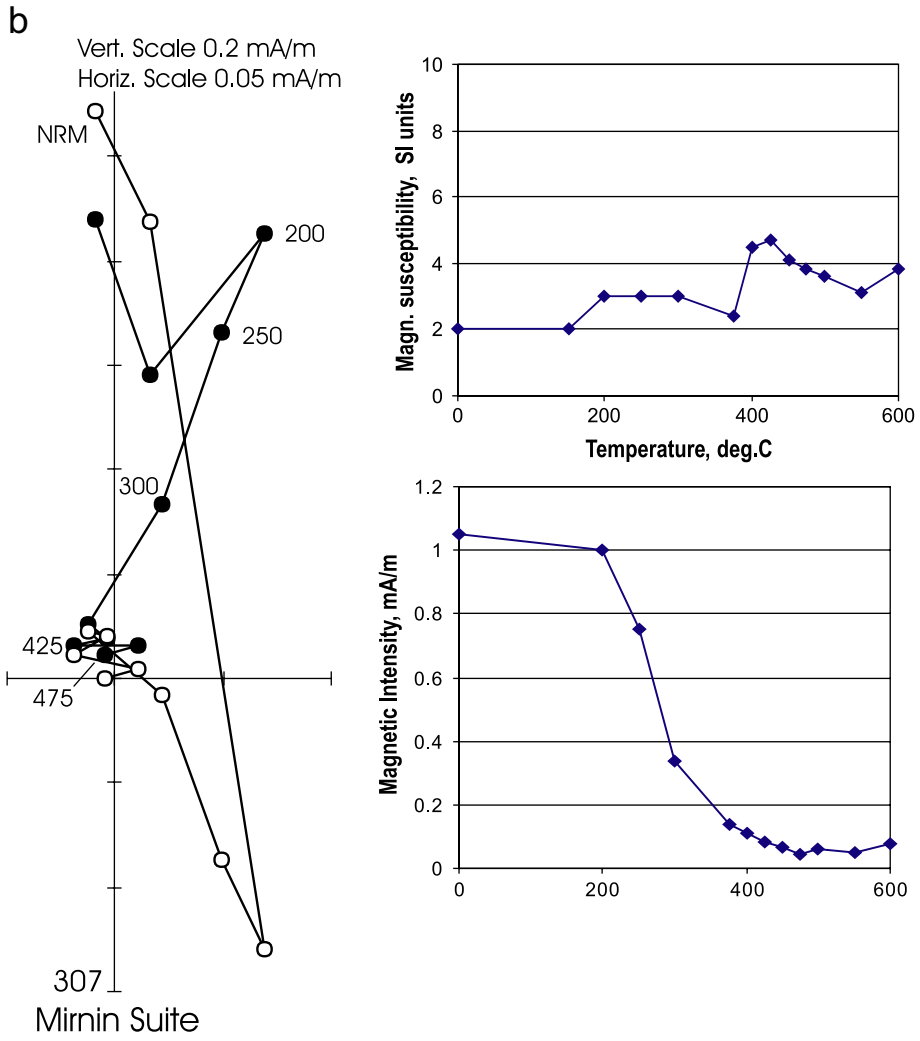

Fig. 3 (*continued*).

river have been studied (Iosifidi, 1988), but most samples displayed thermo-chemical alteration during heating for thermal demagnetization that made it uncertain whether the characteristic magnetizations had been isolated. Samples from the southern part of the uplift (Omulevka river) were used for magnetostratigraphic studies, but the final results include secondary magnetizations, thus were not useful for determining pole positions (Kolosev, 1981, 1995).

Sampling locations for this study are located along the Taskan river and its tributaries in the southwestern part of the Omulevka uplift (Fig. 2), and belong to the Taskan structural province of Merzlyakov (1971) and Gagiev (1996). The geology of the region consists mainly of folded Paleozoic rocks. The folds are generally isoclinal and are often displaced by thrust faults. Many intrusive rocks have been mapped over the whole region, with ages ranging from mid-Jurassic to mid-Cretaceous. Care was taken when selecting paleomagnetic collecting sites to avoid being in close proximity with known intrusive bodies. In all cases, we found a steeply dipping magnetic overprint, but in many sites we were also able to isolate a characteristic

Table 1
Locality data sets

(a) Mirnin, S-2, loc. 6

Sample	Lab.	D_s	I_s	Bed. Az	Bed. Dip
307	UAF	353.4	− 38.6	274	36
309	UAF	302.3	− 32	269	20
310	UAF	316.1	− 41.5	283	28
310	NEISRI	305	− 33	283	28
311	UAF	302.1	− 27.3	269	42
311	NEISRI	310	− 22	269	42
312	UAF	315.4	− 26.4	284	48

Site long.	Site lat.	Mean D_s	Mean I_s	N	κ_s
149.51	63.45	313.9	− 32.5	7	25.4

(b) Nelyudim, D-1, loc. 5

Sample	Lab.	D_s	I_s	Bed. Az	Bed. Dip
293	UAF	355	− 52	259	60
294	UAF	336	− 24	256	55
295	UAF	268	− 36	253	50
296	UAF	345.4	− 50.1	259	60
297	UAF	321	− 51	265	50
301	UAF	267	− 47	251	64

Site long.	Site lat.	Mean D_s	Mean I_s	N	κ_s
149.5	63.46	315.2	− 49.1	6	7.9

(c) Huilchan, D-1, loc. 4

Sample	Lab.	D_g	I_g	Bed. Az	Bed. Dip
222T	UAF	276.8	86.5	263	40
223T	UAF	2.9	77.9	263	40
224T	UAF	81.3	78.4	257	58
225T	UAF	72.9	85.9	266	39
226T	UAF	295	81.4	253	40
227T	UAF	53.8	72.7	253	57
230T	UAF	192.8	79.5	259	58
231T	UAF	31.5	75.6	259	58
232T	UAF	199.4	84.3	259	58
238T	UAF	71.9	87.4	253	45
243T	UAF	276.2	85.3	284	57
245T	UAF	180.4	88.8	294	65
246T	UAF	222.5	85.4	294	65
247T	UAF	22.9	86.5	294	65

Site long.	Site lat.	Mean D_s	Mean I_s	N	κ_s
149.49	63.47	34.7	87.8	14	83.5

(d) Voyakh, D-2, loc. 7

Sample	Lab.	D_s	I_s	Bed. Az	Bed. Dip
337	NEISRI	334.2	− 44.5	129	75
338	UAF	295.6	− 53.3	129	75
339	UAF	289.3	− 31.6	129	75

Table 1 (*continued*)

(d) Voyakh, D-2, loc. 7

Sample	Lab.	D_s	I_s	Bed. Az	Bed. Dip
340	UAF	308.4	− 52.7	129	75
341	UAF	299	− 54.5	129	75
342	NEISRI	334	− 34	129	75

Site long.	Site lat.	Mean D_s	Mean I_s	N	κ_s
149.56	63.48	310.8	− 46.7	6	21.6

(e) Mylgin, D-2, loc. 3

Sample	Lab.	D_s	I_s	Bed. Az	Bed. Dip
141A	UAF	322.4	− 47.9	100	38
141T	UAF	353.1	− 71.9	100	38
142T	UAF	354	− 48.4	94	38
143T	UAF	340.5	− 51	59	44
144T	UAF	312.3	− 50.3	69	55
145T	UAF	318.3	− 58.1	74	42
145A	UAF	306.3	− 32.3	74	42
147A	UAF	316.6	− 55.1	41	12
147T	UAF	326.9	− 38.9	41	12
148T	UAF	339.3	− 66	79	42
149A	UAF	275	− 41	73	35
149T	UAF	311.3	− 62.2	73	35
150A	UAF	313.8	− 40.8	84	47
150T	UAF	346.8	− 52.3	84	47
152A	UAF	304.8	− 54.6	74	30
152T	UAF	331.3	− 62.2	74	30
153T	UAF	345.6	− 56.7	41	45

Site long.	Site lat.	Mean D_s	Mean I_s	N	κ_s
149.46	63.66	322.7	− 54.1	17	25.1

(f) Chara, D-3, loc. 1

Sample	Lab.	D_s	I_s	Bed. Az	Bed. Dip
114	UAF	356	− 48	29	13
117	UAF	351	− 30	5	24
118	UAF	277	− 63	44	4
119	UAF	329	− 69	84	14
120	UAF	339	− 62.7	46	19
122	UAF	322	− 44	354	16

Site long.	Site lat.	Mean D_s	Mean I_s	N	κ_s
149.43	63.79	333.7	− 55.4	6	14.4

(g) Kiprei, C-1, P-2, loc. 1

Sample	Lab.	D_s	I_s	Bed. Az	Bed. Dip
72	UAF	261.3	− 55.2	359	44
73	UAF	239.7	− 64.9	341	51
77	UAF	235.3	− 67	331	48
78	UAF	236.9	− 74.8	347	41

Table 1 (*continued*)

(g) Kiprei, C-1, P-2, loc. 1

Sample	Lab.	D_s	I_s	Bed. Az	Bed. Dip
79	UAF	241.7	− 55.4	339	55
80	UAF	271	− 50.9	347	54
81	UAF	254.1	− 56.7	344	50
85	UAF	236.6	− 37.8	311	35
72	NEISRI	308.2	− 62.3	359	44
73	NEISRI	240.7	− 57.1	341	51
77	NEISRI	246.3	− 55.5	331	48
78	NEISRI	264.3	− 65.2	347	41
80	NEISRI	260.9	− 51.1	339	55
81	NEISRI	256.4	− 61.4	347	54
82	NEISRI	247.1	− 62	341	56
83	NEISRI	235	− 51	325	50

Site long.	Site lat.	Mean D_s	Mean I_s	N	κ_s
149.43	63.81	251.7	− 59.2	16	41.3

(h) Turin, P-2, loc. 1

Sample	Lab.	D_s	I_s	Bed. Az	Bed. Dip
91	UAF	261.8	− 63.3	345	42
92	UAF	240.5	− 62.1	341	46
99	UAF	174.3	− 62.3	326	51
99	NEISRI	246	− 56	326	51
100	UAF	243.8	− 63.8	338	37
100	NEISRI	271	− 63	338	37
101	UAF	196.4	− 55.2	335	65
103	UAF	250.3	− 52.1	333	45
103	NEISRI	224	− 50	333	45
104	UAF	248.2	− 56.3	345	40
104	NEISRI	215	− 63	345	40
105	UAF	265	− 55	359	54

Site long.	Site lat.	Mean D_s	Mean I_s	N	κ_s
149.43	63.81	237.3	− 61.3	12	29.5

For each suite (e.g. Mirnin), the age (S-2) and map location (loc. 6) and the samples for which a characteristic magnetization direction was identified is listed, together with the laboratory in which the measurements were made (University of Alaska, UAF and Northeast Interdisciplinary Scientific Research Institute in Magadan, NEISRI). *D* and *I* are the declination and inclination of the resultant magnetizations. For all suites other than Huilchan, the data are in stratigraphic (tilt corrected) coordinates (D_s, I_s). Huilchan is in geographic coordinates (D_g, I_g) as no pre-tilting magnetization was seen. The Azimuth and angle of dip are noted for the bedding for each sample (Bed. Az, Bed. Dip). For each location, the site longitude (°E) and latitude (°N) are shown together with the mean values of *D* and *I*, the number of samples (*N*) and the Fisher parameter kappa (κ) (Fisher, 1953).

magnetization. For this study, samples of Silurian, Devonian, Carboniferous and Permian rocks were collected.

3. Paleomagnetic sampling and laboratory treatment

Orientated hand samples were collected from each of the eight suites described below. Orientations were made using magnetic compass bearings, with the local magnetic declination being calibrated against map bearings. Each oriented hand sample was cut into four to five cubes $2 \times 2 \times 2$ cm. These samples were then divided into two groups; one analyzed at the paleomagnetic laboratories of the Geophysical institute of the University of Alaska and the other at the laboratories of the Northeast Interdisciplinary Scientific Research Institute (NEISRI), Magadan. All samples were progressively demagnetized using thermal and alternating magnetic field techniques. The magnetization of the samples was measured in a magnetically shielded room at the university of Alaska using a two-axis 2-G cryogenic magnetometer (noise level 1×10^{-5} mA/m), and using a JR-4 spinner magnetometer at NEISRI (noise level 5×10^{-5} mA/m). Magnetic susceptibility was measured with either a Bartington susceptibility meter or a kappa bridge KLY-2.

Demagnetization data were plotted on orthogonal vector diagrams (Zijderveld, 1967) and their characteristic remanent magnetizations (ChRM) were determined using a line-fitting technique (Kirschvink, 1980) on final linear segments that were defined by three or more points including cases where the final component was represented by two points and the origin.

In our analysis of the demagnetization data, the lowest temperature or lowest coercivity component was labeled the A-component. If another higher temperature or coercivity component was seen, this was labeled the B-component. If the final component appeared to be tracking towards the origin of a Zijderveldt diagram, then it was called the ChRM.

4. Local geology and paleomagnetism

4.1. Upper Silurian

4.1.1. Mirnin suite

These rocks are exposed along the right bank of the Taskan river (location 6, Fig. 2) and consist of

interbedded gray, thin-platy limestone, banded calcareous sandstone, marls and sometimes light-gray siltstones and argillites. This suite is considered to be late Ludlovian–Pridolian (approx. 414 Ma) (note that all numerical ages follow the timescale of Harland et al., 1990) based on correlations with the *Neocucullograptinae* to *Pristiograptus* graptolite scale (Shilo, 1978) and confirmed by conodont fauna from this suite and from overlapping and underlying sediments in other areas. For example, the bison suite that underlies the Mirnin suite in the Yasachnaya river basin contains early–late Ludlovian conodonts *Kockelella variabitus* wall. (Gagiev, 1987). The Mirnin suite in the Omulevka river basin was the discovery location for the conodonts *eosteinhornensis*, which is the species-index for the Pridolian *eosteinhornensis* zone of the standard conodont scale (Gagiev, 1987). These observations mean that the age of the Mirnin suite is late Ludlovian–early Pridolian (Gagiev et al., 1982; Kachanov et al., 1982).

Mirnin suite samples show several different styles of demagnetization behavior. Most samples display two or three components of magnetization (Fig. 3). The lowest temperature component (with both reversed and normal polarities) was removed at thermal demagnetization temperatures of about 200 °C. This is interpreted to be a viscous magnetization acquired during the storage of samples in the laboratory. After removing the low temperature component, a few samples displayed a single component that decayed to the origin. The majority of the

Table 2
Magnetic components identified for each suite

Age, suite	Magnetization	N	D_s	I_s	κ_s	α_{95}	D_g	I_g	κ_g	α_{95}
S_2 Mirnin	ChRM	7	313.9	−32.5	25.4	12.2	324.1	−10.4	18.3	17,4
D_1 Nelyudim	ChRM?	**6**	**315.2**	**−49.1**	**7.9**	**25.4**	327.0	4.1	7.0	27.4
	A-component	12	349.3	30.2	5.7	20.0	**16.0**	**84.0**	**42.0**	**6.8**
	B-component	**2**	**121.1**	**−80.5**	**77.3**	**28.8**	351.8	−37.9	56.5	33.9
D_1 Huilchan	A-component	14	359.0	38.0	27.2	7.8	**34.7**	**87.8**	**83.5**	**4.4**
	sill of diabase	1	11.3	82.8	–	–	**11.3**	**82.8**	–	–
	sill of diabase	**1**	271.1	76.1	–	–	**271.1**	**76.1**	–	–
D_2 Voyakh	ChRM, basalt	6	**310.8**	**−46.7**	21.6	14.7	262.9	−12.4	21.6	14.7
	A-component, basalt-all samples	6	238.2	35.5	2.5	54.4	2.5	68.7	5.6	31.2
	A-component, basalt, selected	3	217.0	24.9	19.5	28.7	**46.1**	**79.9**	**19.4**	**28.8**
	sedimentary dyke in basalt	1	219.7	26.8	–	–	87.4	74.8	–	–
	red ssts, grits, and argillites.	7	272.7	34.9	1.6	75.7	**72.7**	**75.9**	**76.9**	**6.9**
D_2 Mylgin	ChRM	**17**	**321.7**	**−53.7**	**27.7**	**6.5**	234.2	−77.2	22.6	7.3
	A-component	17	167.7	57.6	15.0	9.5	**320.0**	**82.6**	**34.0**	**6.2**
D_3 Chara	ChRM	**6**	**333.7**	**−55.4**	**14.4**	**18.3**	345.6	−64.5	10.6	21.6
	A-component	9	132.7	79.3	53.9	7.1	**181.8**	**87.4**	**151.9**	4.2
	B-component	9	340.0	−79.6	66.7	6.4	**39.9**	**−83.4**	**113.6**	**4.9**
C_1–P_2 Kiprei, Turin	ChRM	16	**251.7**	**−59.2**	**41.3**	**5.8**	90.5	−72.7	39.8	5.9
	A-component	22	56.1	36.8	17.3	7.7	**23.1**	**80.2**	**28.8**	**5.9**
P_2 Rogachev	ChRM	12	**237.3**	**−61.3**	**29.5**	**8.1**	99.7	−71.6	20.5	9.8

For each locality sampled, the components of magnetization recognized in the Zijderfeldt plots are listed. ChRM is the most stable vector that decays towards the origin. A-component is the first component recognized during demagnetization, and the B-component the next if it is not the ChRM. The individual components are shown where N is the number of samples used to determine the component, D_s and I_s are the declination and inclination in stratigraphic coordinates together with the value of κ_s and α_{95} after Fisher (1953). The components are also given in geographic coordinates (D_g, I_g, κ_g, α_{95}). The data shown in bold represent measurements that are clearly pre-folding (stratigraphic coordinates) and post-folding (geographic coordinates).

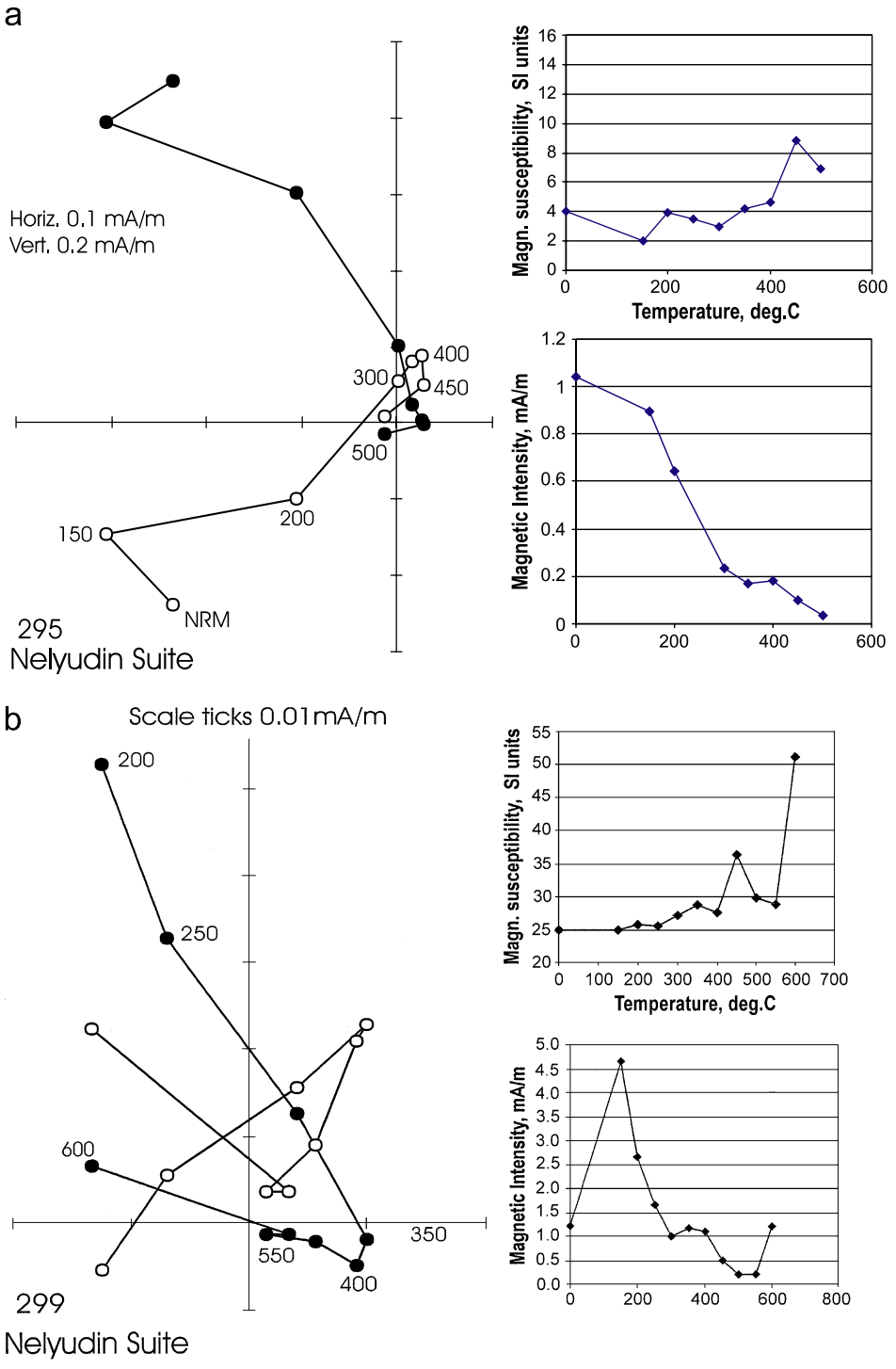

Fig. 4. Demagnetization plots for samples from the Nelyudim suite of lower Devonian age. See caption for Fig. 3 for explanation of symbols. (a) Sample 295, (b) sample 299.

Mirnin suite samples showed an intermediate component that has blocking temperatures of about 350 °C (Fig. 3a). The removal of this intermediate component left a single magnetization with a straight-line decay to the origin of the vector diagram. During high temperature demagnetization, some samples showed changes in directions and intensity of magnetization, but did not decrease towards the origin of the vector diagram (Fig. 3b). However, the directions of magnetizations on separate steps are similar to the direction of the high temperature components seen in the more stable specimens described above. We interpret the high temperature directions to represent the reversed polarity characteristic magnetization that was acquired close to the time of deposition. The samples in this Silurian section are from exposures in a monocline with low variation in bedding attitude, so no definitive fold test was possible; however, the precision parameter kappa (Fisher, 1953) of the characteristic magnetization is greater in stratigraphic ($K=25.4$) than in geographic coordinates ($K=18.3$) (Tables 1a and 2).

4.2. Devonian

4.2.1. Lower Devonian

Two stratigraphic units of lower Devonian age, the Nelyudim and Hiulchan suites, were studied in two different sections.

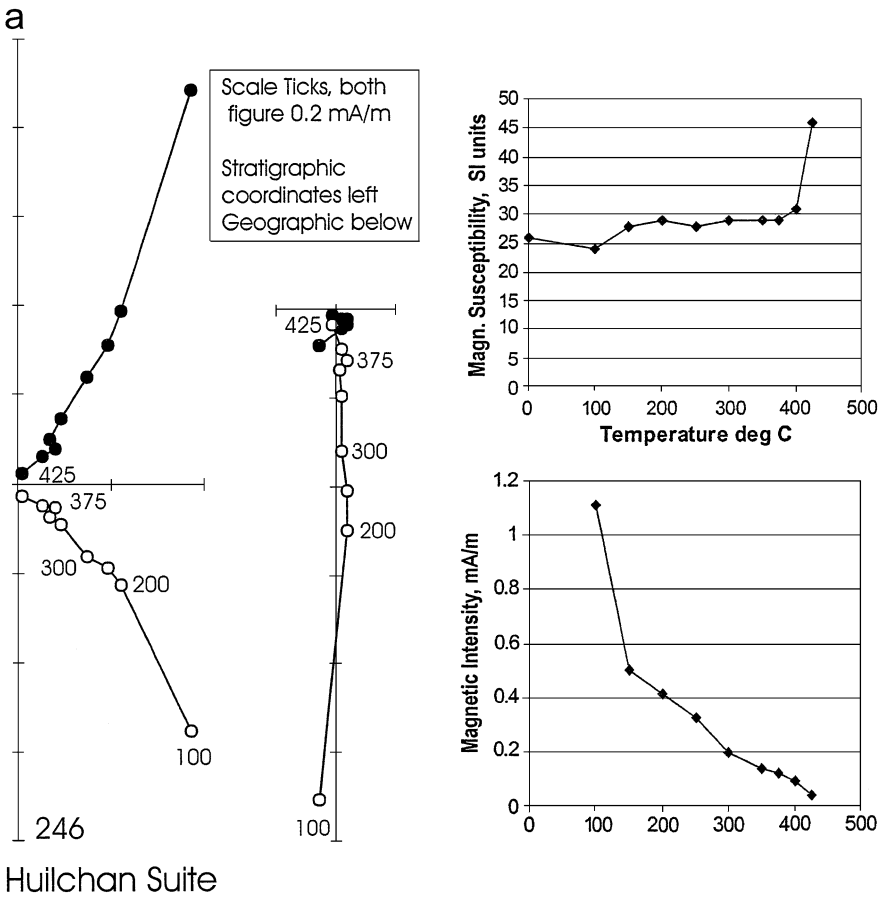

Fig. 5. Demagnetization plots for samples from the Hiulchan suites of lower Devonian age. See caption for Fig. 3 for explanation of symbols. (a) Sample 240, (b) sample 246.

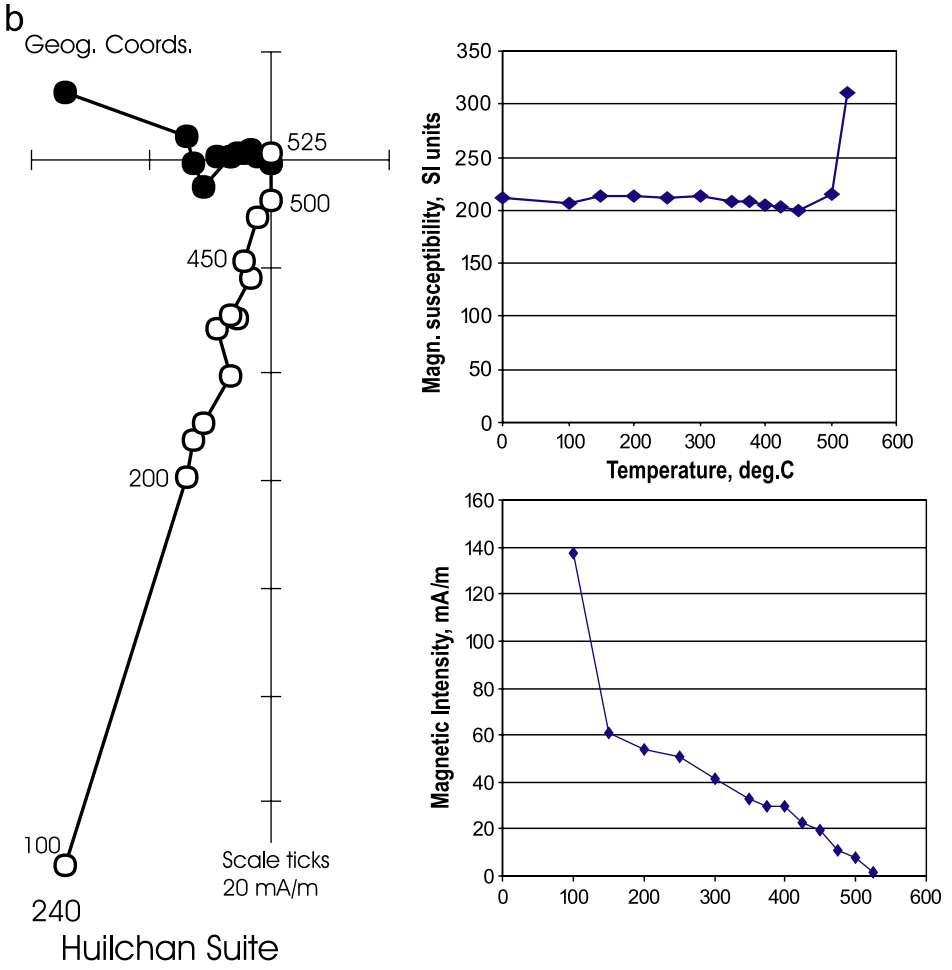

Fig. 5 (*continued*).

4.2.1.1. Nelyudim suite. This suite was also sampled on the right bank of Taskan river (location 5, Fig. 2). This suite is conformable with the underlying Mirnin suite and consists of dark-gray fine-grained limestone. The beds contain fossil corals, algae, gastropods, brachiopods, ostracodes and conodonts. The conodonts belong to zones *remscheidensis*, *repetitor* and *optimus* of the standard conodont scale. The age of the suite is thus correlated with the lower Devonian Lochkovian stage (approx. 400 Ma) (Gagiev, 1996). The rocks of the Nelyudim suite commonly show a single component of magnetization. Almost all intensity is destroyed by about 320 °C, the Curie temperature of pyrrhotite. The magnetization of this component is of normal polarity with a very steep inclination in geographic coordinates and a very low value of kappa in stratigraphic coordinates (Table 2) indicating that the rocks acquired this component after folding. After removing this component, the remaining intensity is very low, but some samples show reversed magnetizations in stratigraphic coordinates (Fig. 4a). These data are listed in Table 1. Two samples show a B-component with reversed directions of magnetization above about 350–400 °C (Fig. 4b).

Because κ_s (5.7) is lower than κ_g (42.0), it is possible that this component was formed before or during folding but the very steep inclinations indicate that it is probably a secondary magnetization. The samples displaying these latter characteristics have

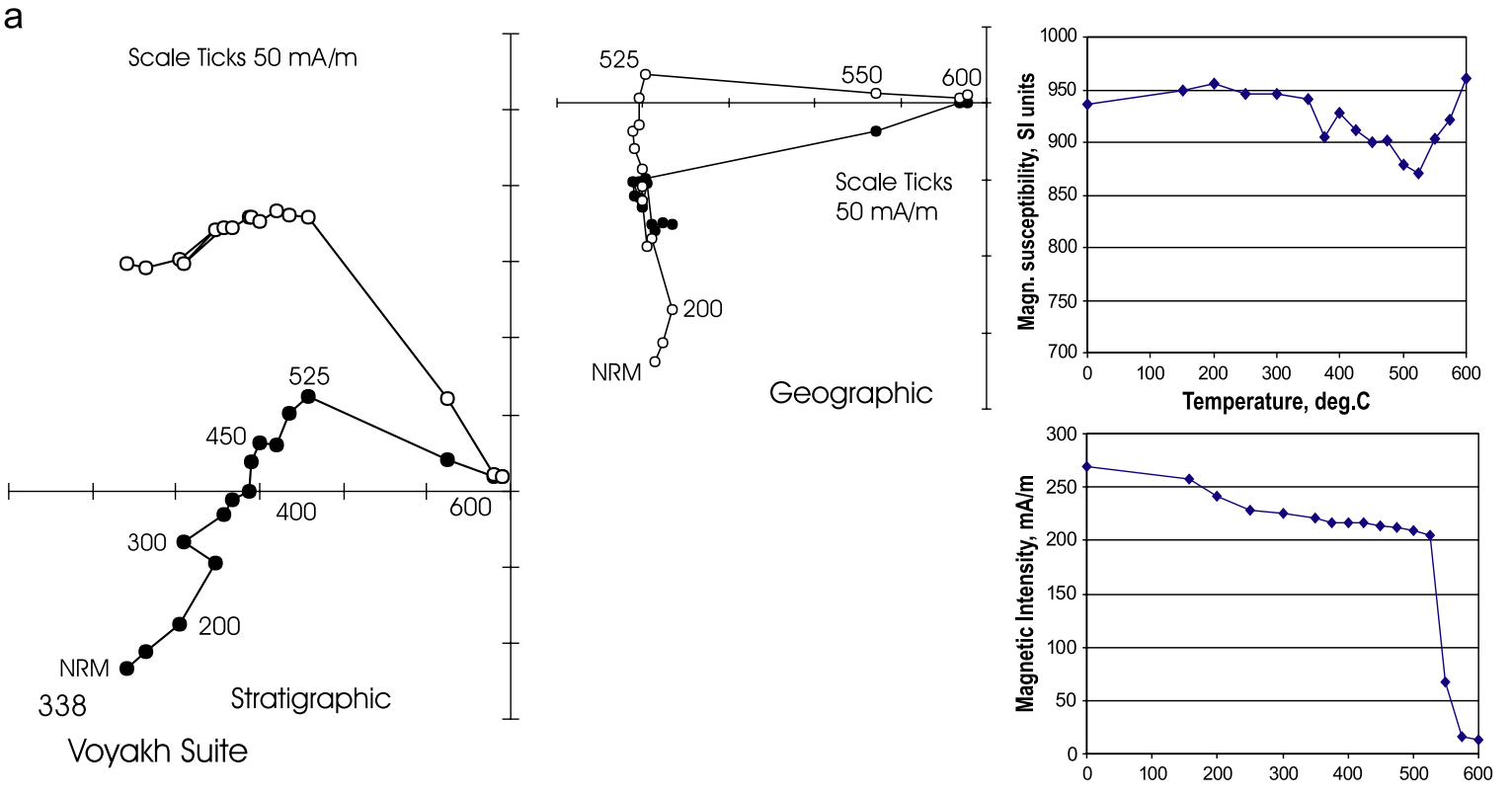

Fig. 6. Demagnetization plots for samples from the Voyakh suite of middle Devonian age. See caption for Fig. 3 for explanation of symbols. (a) Sample 338, (b) sample 344, (c) sample 347.

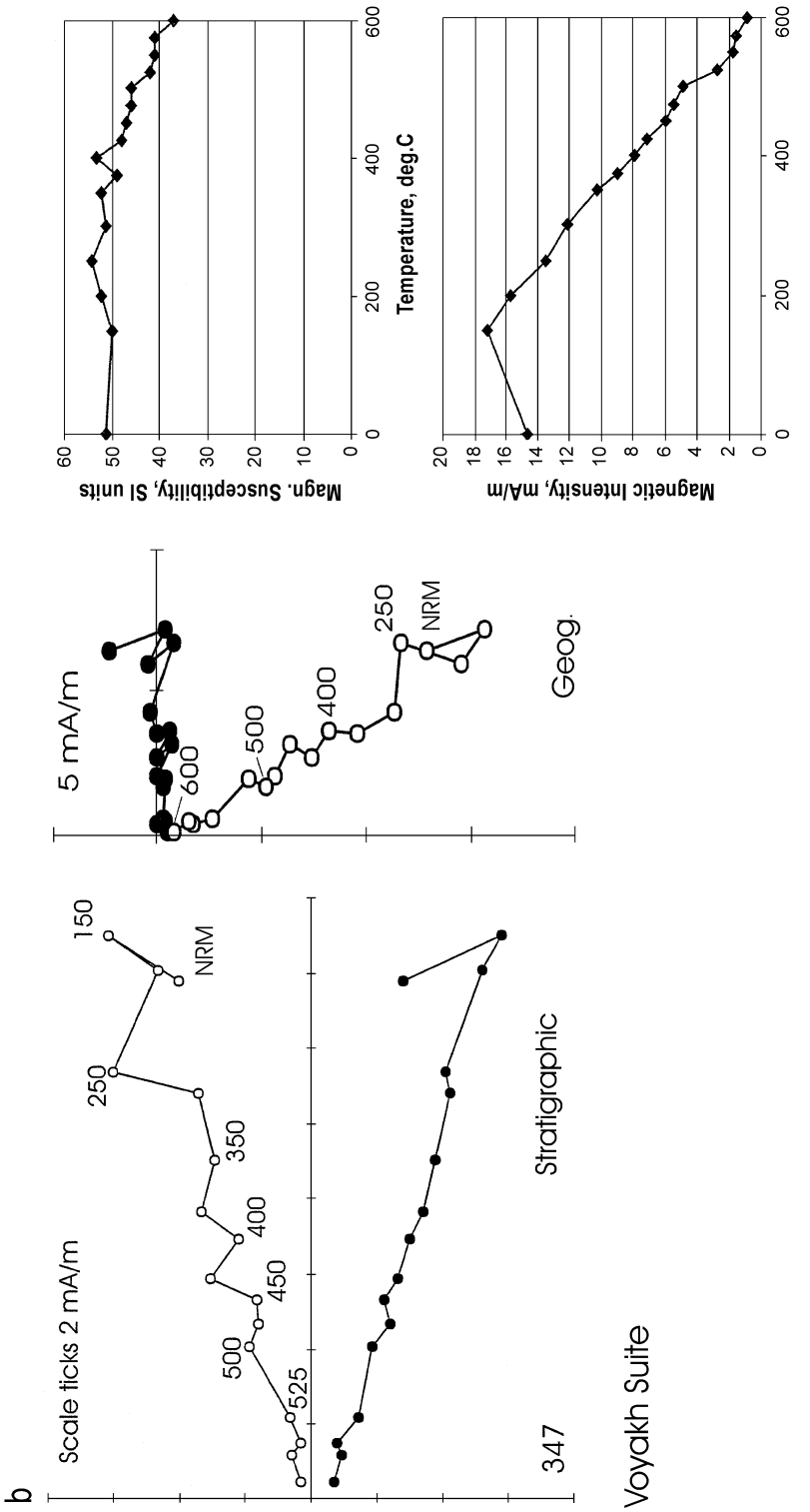

Fig. 6 (*continued*).

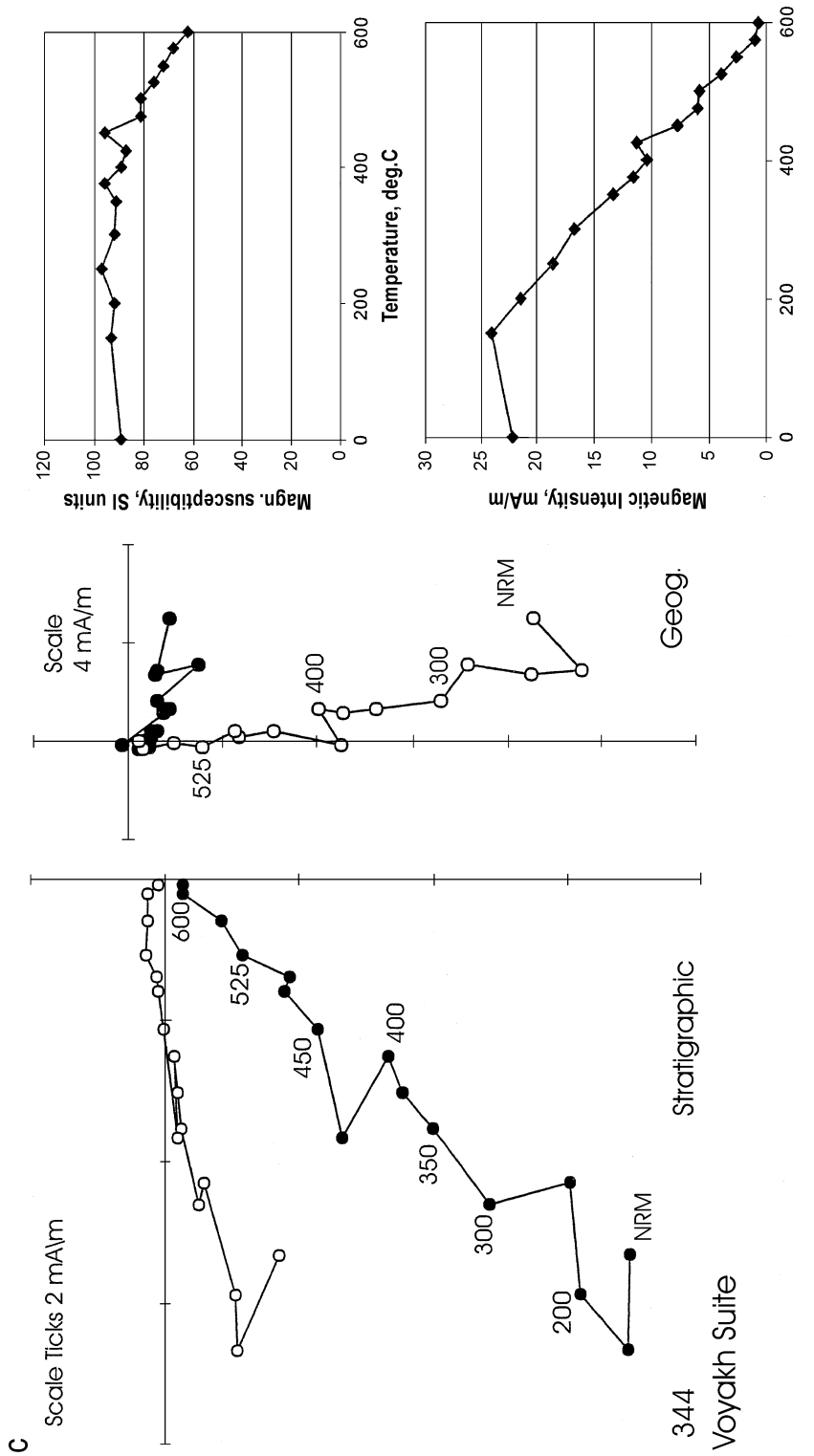

Fig. 6 (*continued*).

anomalously high magnetic susceptibilities and intensities with respect to other samples from this suite, indicating a different magnetic composition.

4.2.1.2. Hiulchan suite. This suite was studied in the Snezhnyi section in the valley of the Snezhnyi creek, a tributary of the Taskan river (location 4, Fig. 1). This suite is composed of intercalations of dark-black siltstone, argillite, and massive and banded limestone. Conodonts found in this section correlate with a range of standard conodont scale zones between *dehiscens* and *patulus* (Gagiev, 1995, 1996), and indicate an age of lower–upper Emsian (approx. 388 Ma).

All samples from this suite are overprinted with a magnetization that commonly persists up to a blocking temperature of 420–425 °C. The overprinted magnetization is usually the only component present. Above about 425 °C, the intensity of magnetization usually drops to near zero (Fig. 5a). In geographic coordinates, the magnetization vectors show northern directions with very steep inclinations. The precision parameter κ has a much higher value in geographic than in stratigraphic coordinates (Table 2) indicating that all samples were overprinted after folding. There are a few thin sills of diabase in this section that only show one component of magnetization (Fig. 5b). This component has a normal polarity with a very steep inclination (Table 2) in geographic coordinates, similar to that seen as the remagnetization component seen in the sediments. This leads to speculation that this part of the section was overprinted by the injection of the sills or by another intrusive body related to the sills.

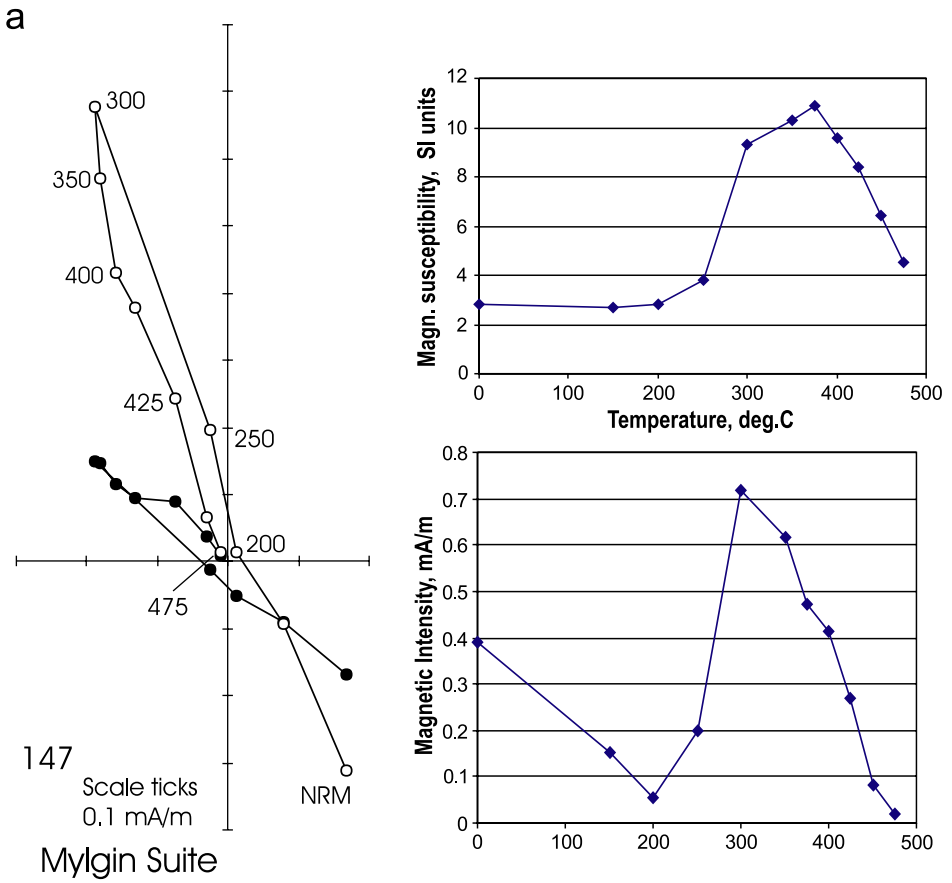

Fig. 7. Demagnetization plots for samples from the Malign suite of middle Devonian age. See caption for Fig. 3 for explanation of symbols. (a) Sample 147, (b) sample 150, (c) sample 152.

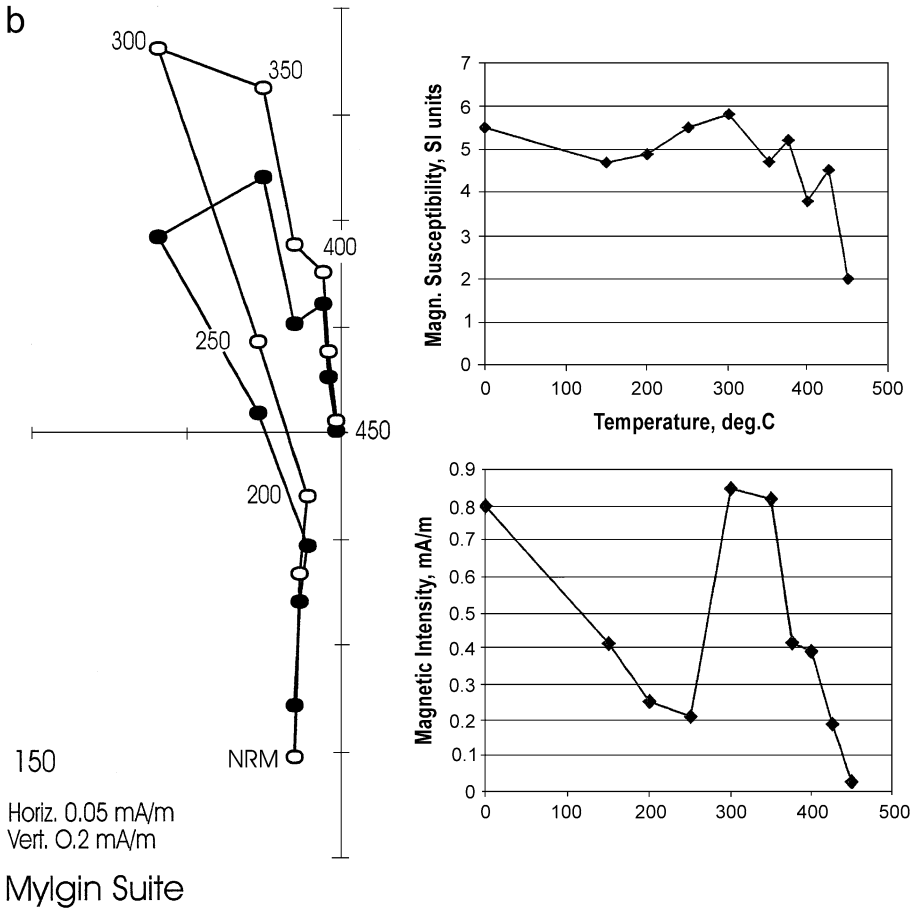

Fig. 7 (*continued*).

4.2.2. Middle Devonian

For middle Devonian time, two stratigraphic sections, the Voyakh and the Mylgin suites, were studied.

4.2.2.1. Voyakh suite. This suite was studied in the Butko basalt and sedimentary section on the left bank of Taskan river, 3 km down from the mouth of Butko river (location 7, Fig. 2). A 5-m-thick, dark green amygdaloidal basalt is exposed in the lower part of the outcrop. The basalt includes injection dykes of red colored dolomitic sandstone. Red colored gritstone, sandstone, siltstone and argillite are exposed on top of the basalt. The sedimentary rocks and basalt belong to the lower part of the Mylgin suite (Shpikerman et al., 1991) or to Voyakh suite that is an analog of Mylgin suite (Gagiev, 1996). Brachiopods *Spinatrypa* ex gr. *aspera* Schoth., *Desquamatia* sp. indet suggest a Middle Devonian age for the suite (Shpikerman et al., 1991). In other locations, correlative rocks contain Givetian conodonts *Polygnathus linquiformis* Hinde, *P.* ex gr. *varcus* Stauf., *icriodus* sp. indet (Shpikerman et al., 1991). The age of the overlapping rocks of Urultun suite is Late Emsian–Lower Eifelian (approx. 386 Ma) (Gagiev et al., 1987).

Basalt flows from the lower part of the Voyakh suite were sampled. These samples generally show two different components of magnetization (Fig. 6a). All but one of the samples gives a reversed polarity before demagnetization. However, the A-component, with blocking temperatures in the range of 500–525 °C, gives a normal polarity with shallow positive

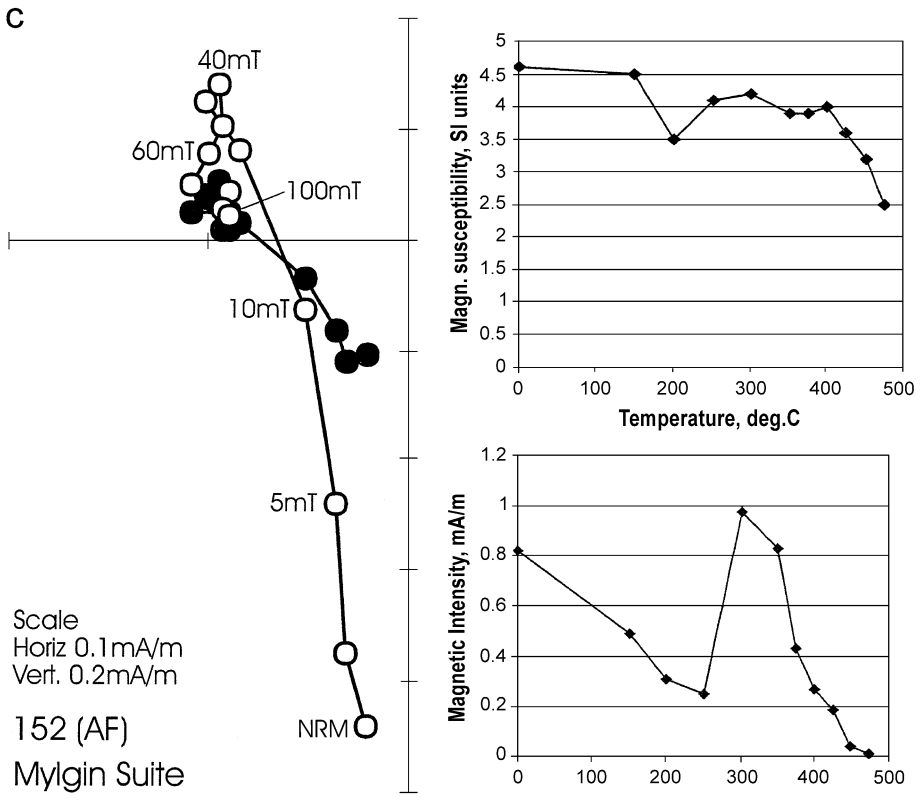

Fig. 7 (*continued*).

inclinations in stratigraphic coordinates and a steep positive inclination in geographic coordinates. In some of the samples, the A-component has a higher relative magnetic intensity than in the others; thus, these directions are considered more reliable indicators of the true direction of A-component (Table 1d). In other samples, progressive demagnetization removed both the A-component and other (characteristic?) components at the same time, but in others the removal of the A-component left a single component that reduced to the origin when plotted on a Zijderfeldt plot (for example, Fig. 6a). The magnetic intensity versus temperature plots (Fig. 6a) indicate that the dominant magnetic carriers are magnetite and hematite, and grains of irregularly shaped hematite are found in these rocks (Shpikerman et al., 1991). The final component, which decays to the origin, is considered to represent the ChRM and is always of reversed polarity (Tables 1d and 2). The demagnetization curves are not typical for basalt, where the original magnetizations are often seen throughout a wide temperature range. The magnetic characteristics obtained here may be a result of strong secondary alterations of basalt. The fact that completely altered and replaced olivine crystals are present together with a lack of dark colored minerals and the appearance of secondary minerals of carbonate, chlorite, mica, epidote, etc. (Shpikerman et al., 1991) indicate significant secondary alteration. The integrated $^{40}Ar/^{39}Ar$ age of the basalt is 177.8 ± 0.9 Ma (Shpikerman et al., 1991). This age is much younger than the stratigraphic age and is presumed to record the time of alteration.

Red sandstone, siltstone and limestone overlap the basalt flows, and are overprinted (Fig. 6b). In stratigraphic coordinates, the magnetic vector directions give both shallow positive and negative inclinations, and declinations that vary from 180° to 270°. These directions are similar to the A-component of magnetization found in the basalt samples. A similar direc-

tion was found in a sample from a sandstone dyke in the basalt (Fig. 6c). In geographic coordinate, these samples have northward directed declinations and steep angles of magnetic inclination (65–80°) (Table 2). We interpret these data as evidence that that the A-component of magnetization of the basalt, and the magnetization of the overlapping rocks were acquired after folding.

4.2.2.2. Mylgin suite. This suite was studied in the valley of Peresokhshii creek, a tributary of the Taskan river (location 3, Fig. 2). This suite is about 450 m thick and consists largely of dark-gray massive dolomite and rare limestone and sandstone. Dolomite in the lower part includes layers of sandstone and clay-limestone, and the middle part is dominated by dolomite breccia. This suite is considered to be an analog of the Voyakh suite and has an age of upper Givetian (approx. 378 Ma) based on conodont data that correlate with the *varcus* zone on the standard conodont scale (Gagiev, 1995, 1996).

These rocks show two clear components of magnetization. Component A has a downward directed inclination and a blocking temperature 300–400 °C. It is removed by alternating field demagnetization in fields of about 40–60 mT and thermal demagnetization temperatures of around 300 °C (Fig. 7a–c). The A-component has a magnetization direction with a very steep positive inclination (82°) in geographic coordinates. The precision parameter is twice as large before tilt correction than after (Table 2). Showing that this component was formed after tilting. After removing the A-component, the magnetization that is left commonly records a reversed component that follows a linear demagnetization path to the origin of a Zijderveldt plot. In most cases, the intensity of magnetization has decreased to near zero by demagnetization temperatures of 450 °C (Fig. 7a). The precision parameter κ for the final demagnetization directions, which are presumed to represent the characteristic magnetization, is higher in stratigraphic than in

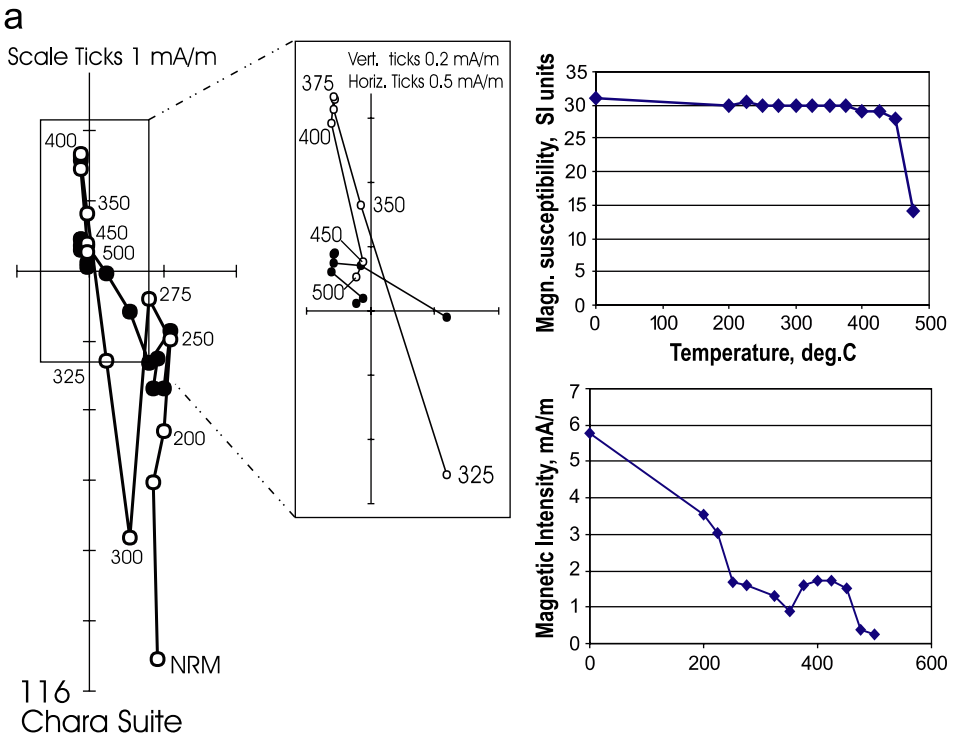

Fig. 8. Demagnetization plots for samples from the Chara suite of upper Devonian age. See caption for Fig. 3 for explanation of symbols. Note expanded center section of plot. (a) Sample 116, (b) sample 118.

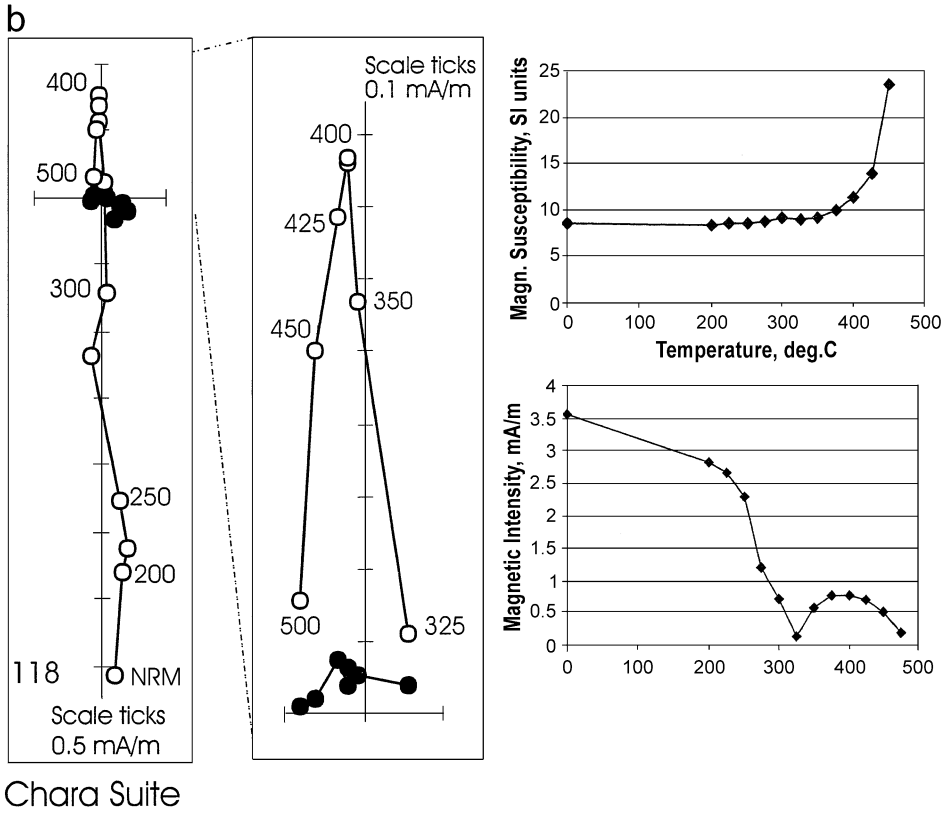

Fig. 8 (*continued*).

geographic coordinates (Table 2). However, the Mylgin rocks are monoclinal where exposed, with very small variations of bedding, and therefore no statistical tilt test is possible. The second component of magnetization is considered to be characteristic. The final direction is similar to that observed in the Voyakh suite.

4.2.3. Upper Devonian

4.2.3.1. Chara suite. This suite (location 2, Fig. 2) lies conformably on the Mylgin suite and is composed of gray limestone, dolomite and rare calcareous sandstone. It has a thickness of about 40 m and contains several fossil types including rugose and tabulate corals, brachiopods, algae and conodonts. The conodonts belong to zones *asymmetricus* and *Anc. triangularis* of early Frasnian age (about 375 Ma).

The rocks sampled in this suite are from monoclinal beds, with shallow dips up to 10°. Samples from this suite are characterized by complicated demagnetization paths on Zijderveld diagrams and, in some cases, up to four components can be distinguished. In some samples, two different normal polarity components were found, one with a blocking temperature of 225 °C, which is a viscous magnetization that was acquired in laboratory, and the other connected with pyrrhotite mineralization. The presence of pyrrhotite could also account for the sharp decreases in intensity that commonly occurs in the 300–325 °C range. In all cases, the A-component is of normal polarity and has blocking temperatures are in the range of 325–400 °C. This component is followed by a component with reversed polarity that persists up to 400 °C, suggesting that this magnetization is now carried by a different magnetic mineral (Fig. 8a,b). Precision parameters, κ, for these two components are much higher in geographic than in stratigraphic coordinates (Table 2) indicating that the component was formed after

tilting. Another component, labeled the B-component, has reversed polarity and very steep inclinations (Table 2) and persists up to 500 °C. The precision parameter (κ) for this component is again much higher in geographic than in stratigraphic coordinates, indicating that component was also acquired after tilting. In general, it is impossible to remove this high temperature component because of strong thermo-chemical alteration of the samples that takes place during heating. The components seen at the highest demagnetization temperatures do not always display a systematic decrease to the origin; however, those seen at temperatures of about 525–500 °C are thought to represent a third polarity change with shallow inclinations and may represent the characteristic direction of magnetization. The mean directions of this magnetization are listed (Tables 1f and 2) but, because they do not show a clear decay towards the origin, they were not used in calculating the final paleopole positions. However, they do provide circumstantial evidence that the internal consistency of the other paleomagnetic directions is real (Table 2). The precision parameters for this high temperature component are greater in stratigraphic than in geographic coordinates (Table 2) indicating that component was formed before tilting.

4.2.4. Upper Carboniferous–Permian

These rocks were studied in a section along the Taskan river, opposite the confluence of the Razgulyai creek tributary (location 1, Fig. 2). The Kiprei, Turin and Rogachev suites were sampled.

4.2.4.1. Kiprei suite. The Kiprei suite forms the lowest member of the middle Carboniferous–Permian section, but only the upper part was studied. The suite consists of about 100 m of interbedded black, dark-gray platy siltstone and green-black platy argillites, with occasional layers of gray limestone. At the present time, fossils have not been discovered in this section; however, brachiopods *Chonotes* cf. *omolo-*

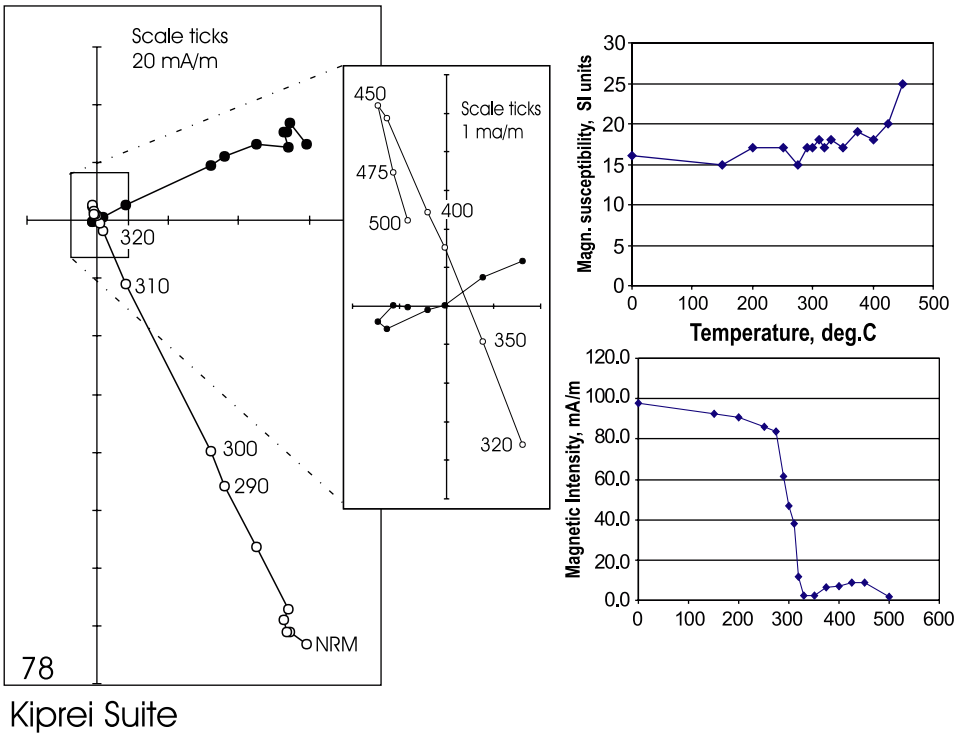

Fig. 9. Demagnetization plots for samples from the Kiprei suite of upper Carboniferous–lower Permian age. See caption for Fig. 3 for explanation of symbols. Note expanded center section of plot.

nensis Lich., *Cancrinella* cf. *cancriniformis* Tschern., *Anidanthus* cf. *rugosus* Lich., *A*. cf. *kuliki* Fred., *Leiorhynchus variabilis* Ustr. et al. are known from exposures of the Kiprei suite in adjacent areas (N.I. Karavaeva, personal communication). The age of the suite is estimated to be Middle Carboniferous–Lower Permian (Geological map of USSR, 1976) or Lower Permian (Shulgina et al., 1999).

4.2.4.2. Turin suite. This suite overlies the Kiprei suite rocks. The Turin suite consists of about 40 m of gray and green-gray thick platy limestone with interbeds of green-gray argillite. The percentage of Argillite increases from the bottom to the upper part of the suite. According to observations made by N.I. Karavaeva (personal communication) Upper Permian *Kolymia* cf. indet and inoceramus bivalves have been found in the upper part of the section, and in other locations Upper Permian *Spiriferella* aff. *ordinaria* Einor, *Cancrinella* ex gr. *repini* Zav., *Anidanthus* sp., *Kolymia inoceramiformis* Lich. have been found.

4.2.4.3. Rogachev suite. The Rogachev suite is conformable with the Turin suite. It is a dark-gray calcareous argillite with rare interbeds of sandy limestone. The suite is about 30 m thick. Because this suite lies on upper Permian rocks and is overlain by lower Triassic rock the age is assumed to be late Permian in age.

All three suites are characterized by similar vector decay diagrams (Figs. 9 and 10). They each contain two oppositely directed components of magnetization. Component A is normally magnetized and has a blocking temperature of 425–450 °C. We interpret he magnetic carriers to be pyrrhotite and magnetite. After removal of this component, the remaining magnetization decays linearly

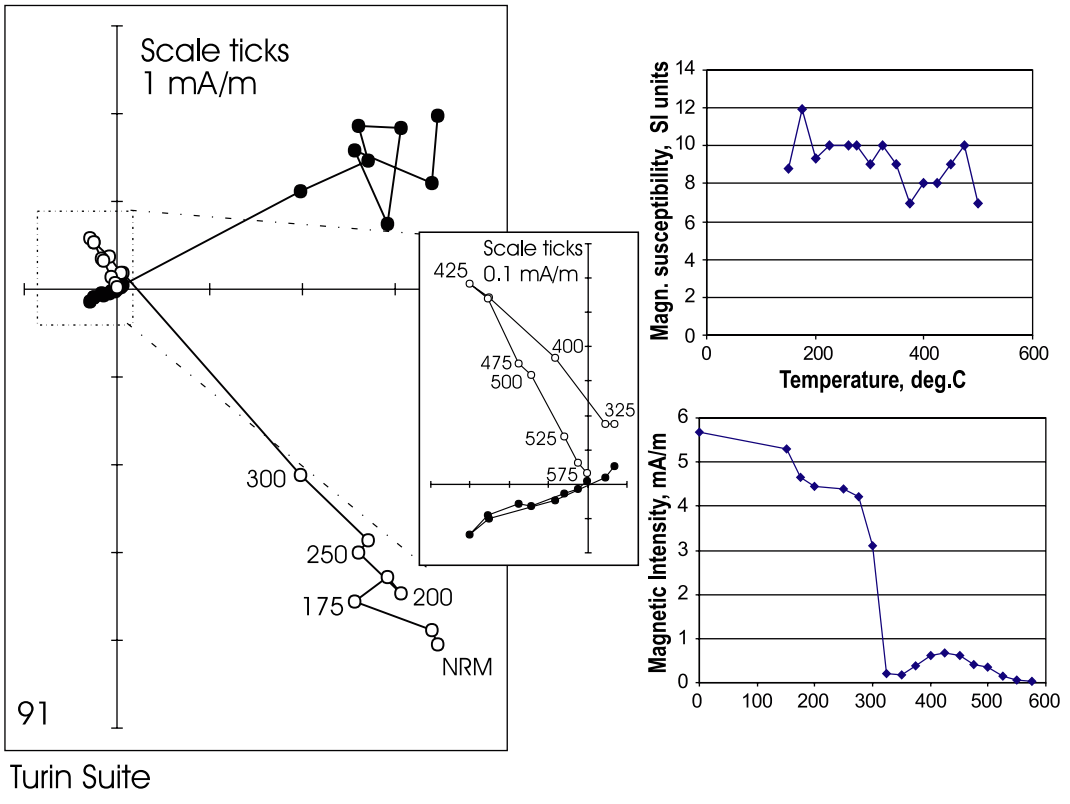

Fig. 10. Demagnetization plots for samples from the Turin suite of upper Permian age. See caption for Fig. 3 for explanation of symbols. Note expanded center section of plot.

Table 3
Bulk magnetic properties

Suite, age	Intensity of NRM (mA/m)			Volume susceptibility in SI units		
	From	To	Average	From	To	Average
Mirnin S_2	0.4	4.1	1.4	1	5	3
Neludim D_1	0.1	4.1	1.0	− 0.3	17.9	3.6
Hiulchan D_1	0.2	12.2	2.3	7	33	25
Voyakh red colored D_2	1.3	41.7	14.4	5	89	39
Voyakh basalt D_2	68.2	563	242.1	105	1069	467
Mylgin D_2	0.04	0.8	0.2	− 0.3	3.9	1.4
Chara D_3	1.2	16.9	4.9	5	15	11
Kiprei C_3–P_1	0.2	795	173.9	9	333	41
Turin P_2	0.9	7.5	4.1	5	16	8
Rogachev P_2	0.7	5.6	3.4	15	162	39

The range of intensities of initial magnetization and volume susceptibility are listed to indicate the overall magnetic characteristics of the sites.

towards the origin. This high temperature magnetic component appears to be carried by magnetite, is reversed and is considered to be the characteristic magnetization (Table 1g,h). Since the rocks sampled are exposed in a monocline with low variations in bedding attitudes, statistical fold or tilt tests cannot be applied. However, the precision parameter for the characteristic magnetization is slightly higher in stratigraphic coordinates than in geographic. The A-component is thought to be due to thermal alteration resulting from nearby intrusive activity. Rocks of the Kiprei suite exposed down-stream from the sites sampled consist of sedimentary rocks cut by small dykes of diabase and by an intrusive body of granite. The sedimentary rocks in this latter section have been heated and mineralized. Sulphide mineralization associated with the granite extends into parts of the Kiprei, Turin and Rogachev suites, as do the older small dykes of diabase. Thermal demagnetization of samples from the diabase dikes shows a magnetic behavior similar to that seen in the mineralized sedimentary rocks. More than 70%

Table 4
Paleopoles of Phanerozoic rocks from the Omulevka terrane characteristic magnetization

Age, suite	D	I	N	κ	α_{95}	Paleolat.	dp	dm	ϕ	λ
S_2 Mirnin	313.9	− 32.5	7	25.4	12.2	17.7	13.8	7.8	− 1.3	192.9
D_1 Nelyudim	315.5	− 49.1	6	7.9	25.4	30	33.6	22.2	10	187.8
D_2 Voyakh	310.8	− 46.7	6	21.6	14.7	27.9	18.9	12.2	9.3	192.2
D_2 Mylgin	321.7	− 53.7	19	27.7	6.5	34.2	9.1	6.3	12.4	181
D_3 Chara	333.7	− 55.4	6	12.8	18.3	35.9	26.1	18.6	11.7	170.8
C_3–P Kip, Tur	251.7	− 59.2	16	41.3	5.8	40	8.7	6.5	43	233.7
P_2 Rogachev	237.3	− 61.3	12	29.5	8.1	42.4	12.5	9.6	51.4	244.6
Overprint										
OP-D_1 Nelud	16.0	84.0	12	42.0	6.8	78.1	13.4	13.2	74.6	161.8
OP-D_1 Huil	34.7	87.8	14	83.5	4.4	85.6	8.8	8.8	67.0	156.0
OP-D_2 Voyb	46.1	79.9	3	19.4	28.8	70.4	55.1	52.7	71.2	198.2
OP-D_2 Voyr	72.7	75.9	7	76.9	6.9	76.9	12.7	11.7	59.2	206.4
OP-D_2 Mulg	320.0	82.6	17	34.0	6.2	75.4	12.1	11.8	72.3	117.3
OP-D_3 Char −	39.9	− 83.4	9	113.6	4.9	77.0	9.6	9.4	52.7	135.5
OP-D_3 Char +	181.8	87.4	9	151.9	4.2	84.8	8.4	8.3	58.4	148.9
OP C_3–P_2	23.1	80.2	22	28.8	5.9	70.9	11.3	10.9	78.6	189.6
Overprint	Mean		8	29.7	10.3				69.5	161.9

The declination and inclination data (D, I, N, κ, α_{95}) are shown together with the resultant paleolatitudes, paleomagnetic pole positions and error limits (Paleolat.); dp, dm (axes of the oval representing the error limits); ϕ (latitude of the pole); λ (longitude of the pole). These are listed for both the characteristic magnetizations (top panel) and the overprints (bottom panel).

of the magnetic intensity is destroyed above 320 °C, which indicates pyrrhotite as the magnetic mineral responsible for this component of magnetization. $^{40}Ar/^{39}Ar$ age for the diabase dyke is 135.2 ± 0.7 Ma (Layer, personal communication) indicating that the secondary magnetization was acquired at this time or later. The mean direction of the secondary magnetization (A-component) is better grouped in geographic than in stratigraphic coordinates showing that the magnetization was acquired after tilting (Table 2). The characteristic magnetizations seen in the sampled sections do not correspond to the overprinting magnetizations associate with the intrusive rocks.

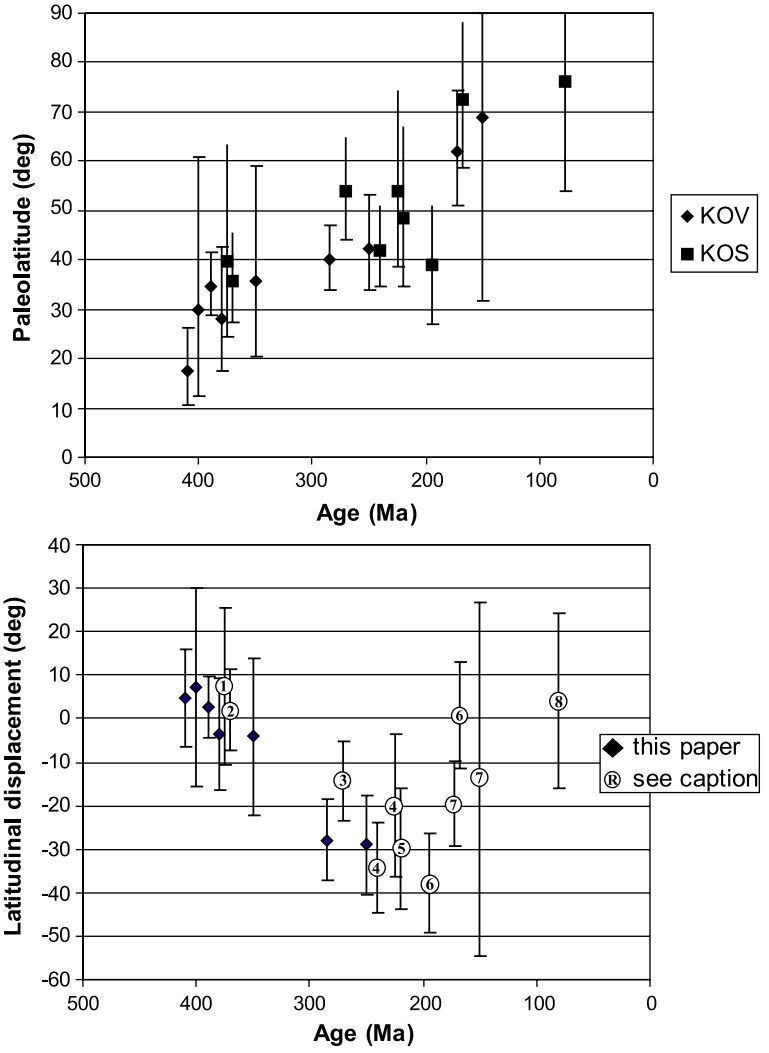

Fig. 11. Paleolatitudes and displacement versus time are shown for the Omolon (KOS) and Omulevka (KOV) terranes. All but the two youngest KOV points are from this study. The paleolatitudes are derived directly from the paleomagnetic inclination data, and the displacement represents the latitudinal difference between the latitude to be expected if the terranes had remained in place (0° displacement) with respect to the Siberian platform. These are obtained by calculating the angular separation of the pole positions for the sampling locations and the equivalent poles taken from the polar wander path for the Siberian platform. The diamond symbol represents data from this study and references for the data with numbered circles are: (1) Kolosev (1981), (2) Kolesov and Stone (2002), (3) Kashik et al. (1990), (4) Khramov (1991), (5) Pechersky (1973), (6) Bondarenko and Didenko (1997).

5. Generalized magnetic properties of the sites sampled

The generalized magnetic properties of the rocks studied show that high magnetic intensities and susceptibilities are typical for the Devonian basalts, but there is a strong heterogeneity of these parameters throughout the basal layer (Table 3). This layer is made up of layers of both massive and amygdaloidal basalt (Shpikerman et al., 1991). The magnetic properties of the Nelyudim, Hiulchan, Voyakh, Turin and Rogachev suites are typical for sedimentary Paleozoic rocks of the Omulevka uplift and have relatively low magnetic intensities and susceptibilities. Rocks of the upper Carboniferous–Permian Kiprei suite show very strong variations of intensity and susceptibility. The high magnetic values in this suite are presumed to be the result of secondary mineralization in these rocks resulting from nearby intrusive activity. Magnetic carriers in these rocks are largely pyrrhotite and magnetite.

6. Discussion and conclusions

We consider that the directions of the characteristic magnetizations obtained from Silurian through early Permian aged rocks were acquired during or shortly after deposition or extrusion, and may be used for geodynamic reconstructions. Because all exposures showed monoclinal bedding and no mixed polarities were seen in the characteristic magnetizations at individual sites, this argument has not been validated statistically. However, a regional comparison between the characteristic magnetizations identified at multiple localities representing Silurian through Devonian time shows that their characteristic magnetizations are quite similar to one another. Many reconstructions place the localities close together throughout this time, and the combined locations show better precision parameters after tilt correction than before. The same arguments hold for the two localities of Permo–Carboniferous age.

It is notable that the paleomagnetic inclination variation correlates with the age of the sampled unit, becoming systematically steeper with decreasing age from Silurian to Permian time (Tables 4 and 5, Fig. 11). It is difficult to imagine a geological process that could overprint all the localities in such a way as to produce this systematic steepening. Based on these observations, we feel it is justifiable to interpret the derived pole positions in terms of paleogeography.

In addition to the ChRM, there are magnetic overprints, all of them almost vertically downward directed in present day coordinates. The dominant overprint is thought to be related to the final accretion of the Kolyma–Omolon superterrane to the Siberian platform. Comparison of the paleomagnetic poles representing the overprint with the equivalent poles for Siberia derived by Besse and Courtillot (1991) indicate a late Jurassic–early Cretaceous field. However, the scatter of the overprint directions seen in this study also hints at a later remagnetization event during late Cretaceous time.

The mean characteristic magnetizations have been used to calculate pole positions for comparison with

Table 5
Displacement and rotation Omulevka terrane with respect to the Siberian craton

Age	Site		Obtained pole				Pole for Siberia			Paleolatitude			Rotation
	Lat	Long	Lat	Long	N	α_{95}	Lat	Long	α_{95}	Lat_{obs}	Lat_{exp}	ΔLat	R
S_2	63.5	149.5	−1.3	192.9	7	12.2	−10	120	9	17.7 ± 12.2	13.1 ± 9	−4.6 ± 11.8	−76.0 ± 12.3
D_1	63.5	149.5	10.0	187.8	6	25.4	−2	130	6	30.0 ± 25.4	22.9 ± 6	−7.1 ± 20.4	−66.0 ± 23.7
D_2	63.5	149.5	9.3	192.2	6	14.7	6	136	4	27.9 ± 14.7	31.6 ± 4	3.8 ± 11.9	−65.1 ± 13.5
D_2	63.6	149.4	12.4	181.0	19	6.5	6	136	4	34.2 ± 6.5	31.6 ± 4	−2.6 ± 6.0	−53.9 ± 7.2
D_3	63.6	149.3	11.7	170.8	6	18.3	14	141	4	35.9 ± 18.3	40.1 ± 4	4.1 ± 14.6	−36.9 ± 18.3
C_3–P_1	63.6	149.3	43.0	233.7	16	5.8	42	158	9	40.0 ± 5.8	67.8 ± 9	27.8 ± 8.5	−90.9 ± 20.2
P_2	63.6	149.3	51.4	244.6	12	8.1	46	161	9	42.4 ± 8.1	71.2 ± 9	28.8 ± 9.6	−96.8 ± 24.6

The latitudes and longitudes of the sites are given along with the paleomagnetic poles for the sites and the equivalent paleomagnetic pole for the Siberian platform. From these, the paleolatitudes and relative rotations of the sites with respect to the Siberian platform have been derived. Lat_{obs} is the observed paleomagnetic paleolatitude for the site. Lat_{exp} is the paleolatitude that would be expected if the sites had remained fixed with respect to the Siberian platform. ΔLat is the relative change or displacement between the sites and the Siberian platform and R is the relative rotation.

the reference poles for the Siberian platform taken from Didenko and Pechersky (1993). In Silurian time, the Omulevka terrane was located at a low paleolatitude, similar to that determined for the Verkhoyansk margin of the Siberian platform (Fig. 11, Table 5) (Didenko and Pechersky, 1993). In post-Devonian time, the Omulevka terrane moved northwards (Figs. 11 and 12, Table 5) initially at the same rate as the equivalent parts of the Siberian platform, then at a lower rate causing a latitudinal separation between them. The maximum latitudinal separation of the Omulevka terrane from the Siberian platform occurred in Permian time. Between Silurian and Permian time, the Omulevka terrane rotated counterclockwise by an angle between 37° and 97°. From Permian to late Jurassic time, the terrane moved steadily northward and simultaneously rotated clockwise (Table 4 and Fig. 12). From latest Jurassic time to the present, the Omulevka terrane has not rotated significantly and has undergone limited horizontal motion with respect to the Siberian craton (Aleksyutin et al., 2001). Paleomagnetic data from the adjacent Omolon terrane show similar paleolatitude changes with time (Kolosev, 1981; Kolesov and Stone, 2002). The combined data sets have been used to produce a paleolatitude versus time curve for these core terranes of the Kolyma–Omolon superterrane (Fig. 11). In recent reconstructions, such as those by Lawver et al. (2002), the

Fig. 12. The apparent polar wander path for eastern Siberia (Didenko and Pechersky, 1993) is shown for comparison with the poles from this study (larger black dots) and those of an earlier study from the Omolon terrane (Kolesov and Stone, 2002).

locations of the terranes that now make up the Kolyma–Omolon superterrane are commonly shown as being nearby the Siberian margin, but in the text it is pointed out that their locations are based on geologic similarities, and the actual locations are very poorly constrained. Adding our data to the reconstructions of Lawver et al. (2002) would place these terranes further south in the proto-Pacific. By late Jurassic time, the amalgamation of the Kolyma–Omolon superterrane was complete and accretion to the Siberian craton with associated folding, thrusting and deformation of the margins had begun. The time of accretion is based on the presence of the collisional granite belts mapped along the northwestern, western and southwestern boundaries of the superterrane. The ages of these granites range from about 180 to 95 Ma (Layer et al., 2001). These conclusions are in accord with those of Didenko et al. (2002), who place the component parts of the Kolyma–Omolon superterrane off-shore from the Verkhoyansk margin of Siberia in late Jurassic time.

Acknowledgements

We would like to acknowledge the financial support received from the U.S. National Science Foundation (grant number OPP95-00241) and the Far East Branch of the Russian Academy of Sciences through NEISRI. We are also grateful to W. Munly and F. Minyuk for help in the field.

References

Aleksyutin, M.V., Bondarenko, G.E., Minyuk, P.S., 2001. Result of structural and paleomagnetic investigations of Jurassic and Cretaceous complexes in mesozoides of NE Russia. Geol. Pac. Ocean 16, 831–852.

Besse, J., Courtillot, V., 1991. Revised and synthetic apparent polar wander paths of African, Eurasian, North American and Indian plates and true polar wander since 200 Ma. J. Geophys. Res. 5 (B3), 4029–4050.

Bondarenko, G.E., Didenko, A.N., 1997. New geologic and paleomagnetic data on the Jurassic–Cretaceous history of the Omolon massif. Geotectonics 31, 99–111.

Burke, K., 1984. Plate Tectonic History of Arctic: MGK, 27th Session, Arctic Geology Section 4, Papers, vol. 4. Nauka, Moscow, pp. 159–167 (in Russian).

Chekhov, A.D., 1990. Structure and Development of the Mesozoides of the Northeast USSR, Part 2. Northeast Interdisciplinary Scientific Research Institute (SVKNII), Magadan. 79 pp. (in Russian).

Didenko, A., Pechersky, D., 1993. Revised Paleozoic apparent polar wander paths for E. Europe, Siberia, N. China and Tarim plates. Prog. and Abstr. for L.P. Zonenshain Memorial Conference on Plate Tectonics, Moscow, Nov., p. 47.

Didenko, A.N., Bondarenko, G.E., Sokolov, S.D., Kravchenko-Berezhnoy, I.R., 2002. Jurassic–Cretaceous history of the Omolon massif, northeast Russia: geologic and paleomagnetic evidence. In: Miller, E.L., Grantz, A., Klemperer, S.L. (Eds.), Tectonic Evolution of the Bering Shelf-Chukchi Sea-Arctic Margin and Adjacent Landmasses. Geol. Soc. Amer. Spec. Paper, vol. 360, pp. 225–241.

Fisher, R.A., 1953. Dispersion on a sphere. Proc.-R. Soc., A 217, 295–305.

Gagiev, M.H., 1987. Stratigraphy and Conodont Lower–Middle Devonian Sediments of North-East USSR. NEISRI FESC RAS, Magadan. 40 pp. (in Russian).

Gagiev, M.H., 1995. Stratigraphy of Devonian and Lower Carboniferous of the Omulevka Uplift (northeastern Asia). NEISRI FEB RAS, Magadan. 196 pp. (in Russian).

Gagiev, M.H., 1996. Middle Paleozoic of North-East Asia. NESC FEB RAS, Magadan. 120 pp. (in Russian).

Gagiev, M.H., Kachanov, E.I., Smirnova, L.V., 1982. Detailed stratigraphic scheme of lower Devonian and boundary with them sediments of Omulevka uplift. Paleontology and Detailed Stratigraphic Correlation. Abstract of XXVIII Session of all Union Paleontology Society: Part 2. Northeast Interdisciplinary Scientific Research Institute, Tashkent, p. 10 (in Russian).

Gagiev, M.H., Rodygin, S.A., Timofeeva, O.B., 1987. Zone Subdivision and Correlation of Lower–Middle Devonian Sediments of Salair and North-East USSR According Conodont Data. NEISRI FESC RAS, Magadan. 56 pp. (in Russian).

Grinberg, G.A., Gusev, G.S., Bakharev, A.G., Bulgakova, M.D., Ipat'eva, I.S., Nedosekin, Yu.D., Rukovich, V.N., Solov'ev, V.N., Surnin, A.A., Tretyakov, F.F., 1981. In: Grinberg, G.A., Rudich, K.N. (Eds.), Tectonic of Magmatic and Metamorphic Complexes of Kolyma–Omolon Massif. Nauka, Moscow. 358 pp. (in Russian).

Harland, W.B., Armstrong, R.L., Cox, A.V., Craig, L.E., Smith, A.G., Smith, D.G., 1990. A Geologic Timescale 1989. Cambridge Univ. Press, Cambridge, p. 263.

Iosifidi, A.G., 1988. New paleomagnetic data on Kolyma massif (Arga–Tas range). Paleomagnetism and Accretion Tectonic. VNIGRI, Leningrad, pp. 104–123 (in Russian).

Kachanov, E.I., Gagiev, M.H., Smirnova, L.V., 1982. New data on lower Devonian and boundary with them sediments of Omulevka uplift (North-East USSR). Pac. Geol., N 4, 79–89 (in Russian).

Karasik, A.M., Ustritsky, V.I., Khramov, A.N., 1984. The history of formation of arctic ocean. 27th International Geologic Congress, Arctic Geology, Colloquium 04, Reports, vol. 4. Nauka, Moscow, pp. 179–189.

Kashik, D.S., Ganelin, V.G., Karavaeva, N.I., Byakov, A.S., Miclukhho-Maclay, O.A., Stukalina, G.A., Lozhkina, N.V., Dorofeeva, L.A., Burkov, J.K., Guteneva, E.I., Smirnova,

L.N., 1990. A Key Permian Section of the Omolon Masif. Pub. bu NAUKA, Leningrad, p. 198.

Khramov, A.N., 1991. Standard paleomagnetic pole range of north Eurasia plates: connection with paleogeodynamic problems of USSR territoty. In: Khramov, A.N. (Ed.), Paleomagnetism and Paleogeodynamics of the USSR Territory. Ministry of Geology of the USSR (VNIGRI), Leningrad, pp. 154–177 (in Russian).

Khramov, A.N., Ustrtitsky, V.I., 1990. Paleopositions of some northern Eurasian tectonic blocks: paleomagnetic and paleobiologic constraints. In: Van der Voo, R., Schmidt, P.W. (Eds.), Reliability of Paleomagnetic Data. Tectonophysics, vol. 184, pp. 101–109.

Khramov, A.N., Gurevich, E.L., Komissarova, R.A., Osipova, E.P., Pisarevski, S.A., Rodionov, V.P., Slautsitais, I.P., 1985. Paleomagnetism, microplates and Siberian plate consolidation. J. Geodyn. 2, 127–139.

Kirschvink, J.L., 1980. The least-square line and plane and the analysis of paleomagnetic data. Geophys. J. Astron. Soc. 62, 699–718.

Kolesov, E.V., 1995. Magnetostratigraphy of reference sections of upper Silurian and lower Devonian of central regions of Kolyma. Magnetostratigraphic Study of Phanerozoic. NEISRI FEB RAS, Magadan, pp. 12–17 (in Russian).

Kolesov, E.V., Stone, D.B., 2002. Paleomagnetic paleolatitudes for upper Devonian rocks of the Omolon massif, northeast Russia. In: Miller, E.L., Grantz, A., Klemperer, S.L. (Eds.), Tectonic Evolution of the Bering Shelf-Chukchi Sea-Arctic Margin and Adjacent Landmasses. Geol. Soc. Amer. Denver, CO, Spec. Paper, vol. 360, pp. 243–257.

Kolosev, E.V., 1981. Paleomagnetic characteristics of middle Paleozoic sediments of the Omolon massif. Magnetism of Rocks and Paleomagnetic Stratigraphy in Eastern and Northeastern Asia. Northeast Interdisciplinary Scientific Research Institute, Magadan, pp. 68–74.

Lawver, L.A., Grantz, A., Gahagan, L.M., 2002. Plate kinematic evolution of the present Arctic region since the Ordovician. In: Miller, E.L., Grantz, A., Klemperer, S.L. (Eds.), Tectonic Evolution of the Berin Shelf-Chukchi Sea-Arctic Margin and Adjacent Landmasses. Geol. Soc. Amer. Denver, CO, Spec. Paper, vol. 360, pp. 333–358.

Layer, P.W., Newberry, R., Fujita, K., Parfenov, L., Trunilina, V., Bakharev, A., 2001. Tectonic setting of the tectonic belts of Yakutia, northeast Russia, based on $^{40}AR/^{39}AR$ geochronology and trace element geochemistry. Geology 29 (2), 167–170.

Merzlyakov, V.M., 1966. On stratigraphy of Carboniferous and Permian sediments of southwestern part of Omulevka mounts. Proceeding on Geology and Ore Minerals of North-East USSR. Magadan, vol. 19, pp. 3–10 (in Russian).

Merzlyakov, V.M., 1971. Stratigraphy and Tectonic of Omulevka uplift. M: Nauka (152 pp., in Russian).

Merzlyakov, V.M., 1986. Geology of central parts of North-East USSR. Dissertation for degree of doctor Mineralogy–Geology, Novosibirsk, p. 32 (in Russian).

Merzlyakov, V.M., Terekhov, M.I., Lychagin, P.P., Dulevsky, Ye.F., 1982. Tectonics of the Omolon massif. Geotectonics, N 1, 74–86 (in Russian).

Minyuk, P.S., Kolesov, E.V., Stone, D.B., Ivanov, Yu., 2001. Preliminary paleomagnetic study results for Paleozoic sequences of the Omulevka uplift, in northeastern Asia. Paleomagnetic and Magnetic Rock Studies in the North-East of Russia. NEISRI RAS, Magadan, pp. 31–40 (in Russian).

Nikolaev, A.A. (Ed.), 1976. Geological map of USSR. Sheet P-55-VI-Upper stream of Taskan river. Scale 1:200 000. Explanation note. AirGeology, Moscow. 83 pp.

Nokleberg, W.J., West, T.D., Dawson, K.M., Shpikerman, V.I., Buntdzen, T.K., Parfenov, L.M., Monger, J.W.H., Ratkin, V.V., Baranov, B.V., Byalobzhesky, S.G., Diggles, M.F., Eremin, R.A., Fujita, K., Gordey, S.P., Gorodinskiy, M.E., Feeney, N.A., Frolov, Y.F., Grantz, A., Khanchuk, A.I., Koch, R.D., Natal'in, B.A., Natapov, L.M., Norton, I.O., Patton, W.W., Plafker, G., Pozdeev, A.I., Rozenblum, I.S., Scholl, D.W., Sokolov, S.D., Sosunov, D.M., Stone, D.B., Tabor, R.W., Tsukanov, N.V., Vallier, T.L., 1998. Summary terrane, mineral deposits, and metallogenic belt maps of the Russia Far East, Alaska and the Canadian Cordillera. U.S. Geol. Survey Open File Report, No.98-136, CD-ROM.

Nokleberg, W.J., Parfenov, L.M., Monger, J.W.H., Norton, I.O., Khanchuk, A.I., Stone, D.B., Scholl, D.W., Fujita, K., 2001. Phanerozoic tectonic evolution of the Circum-North Pacific. U. S. Geol. Surv. Prof. Pap. 1626, 122.

Parfenov, L.M., 1984. Continental Margins and Island Arcs of the Mesozoides of Northeast Asia. Nauka, Novosibirsk, p. 192 (in Russian).

Parfenov, L.M., 1991. Tectonics of the Verkhoyansk–Kolyma Mesozoides in the context of plate tectonics. Tectonophysics 199, 319–342.

Pechersky, D.M., 1973. Paleomagnetic directions and pole positions: Data for the USSR-Issues 2 and 3, Soviet Geophysical Committee: World Data Center-B (Moscow), Catalog.

Shapiro, M.N., Ganelin, V.G., 1988. Paleotectonic correlations of the large blocks in mesozoides of the USSR North-East. Geotectonics, N 5, 94–104 (in Russian).

Sharkovsky, M.B., 1975. Tectonics of the Kolyma–Indigirka interfluve. Geotectonics, N 6, 44–60 (in Russian).

Shilo, N.A. (Ed.), 1978. Proceeding of II Stratigraphic Meeting on Precambrian and Phanerozoic North-East USSR (Magadan, 1974–1975). Northeast Interdisciplinary Scientific Research Institute, Magadan, p. 192 (in Russian).

Shpikerman, V.I., Shpikerman, L.A., Volkov, M.N. (Eds.), 1991. Middle Devonian cupriferous basalt of South of Omulevka uplift. Proceeding on Geology and Ore minerals of North-East USSR. Magadan, vol. 27, pp. 183–190 (in Russian).

Shulgina, V.S., Tkachenko, V.I., Gagiev, M.H., et al., 1999. Legend of Kolyma Series Sheets of State Geological Map of Russian Federation of scale 1:200 000 (issue 2). M.: GNPP "AirGeology". p. 42.

Talent, J.A., 1990. Interrelations among lithological blocks on north-east of the USSR: autochthonous or newcomer from far away? Geotectonics N2, 123–125 (in Russian).

Til'man, S.M., 1973. Comparative Tectonics of the Mesozoides of the Northern Pacific Ring. Nauka, Novosibirsk. 326 pp. (in Russian).

Ustritsky, V.I., Khramov, A.N., 1987. On the history of formation of northern part of Pacific ocean and the Pacific mobile belt (com-

parison of paleomagnetic and paleobiogeographical data from the adjacent land). Essays on the Geology of the Northwestern Sector of Pacific Tectonic Belt. Nauka, Moscow, pp. 239–276 (in Russian).

Zijderveld, J.D.A., 1967. A.C. demagnetization of rocks. In: Collinson, D.W., Creer, K.M., Runcorn, S.K. (Eds.), Methods in Palaeomagnetism. Elsevier, New York, pp. 256–286.

Zonenshain, L.P., 1984. Tectonics of the inner continental folded belts. 27th International Geologic Congress, Tectonics, Colloquium 07, Papers, vol. 7. Nauka, Moscow, pp. 48–59 (in Russian).

Zonenshain, L.P., Kuzmin, M.I., Natapov, L.M., 1990a. Tectonics of the Lithosphere Plates of the USSR, Book 2. Nedra, Moscow. 334 pp. (in Russian).

Zonenshain, L.P., Kuzmin, M.I., Natapov, L.M., 1990b. Geology of the USSR: a plate-tectonic synthesis. Page, B.M. (Ed.), Amer. Geophys. Union Geodynamic Series, vol. 21. 242 pp.